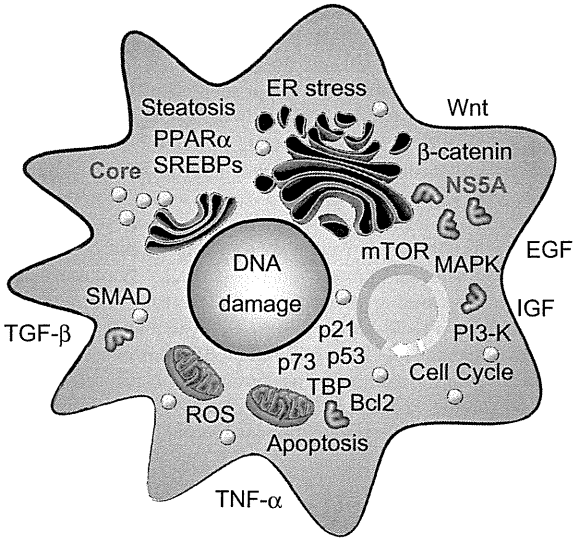

Figure 1 Signaling pathways potentially affected by hepatitis C virus (HCV) proteins. EGF, epidermal growth factor; ER, endoplasmic reticulum; IGF, insulin-like growth factor; MAPK, mitogen activated protein kinase; mTOR, mammalian target of rapamycin; PI3-K, phosphatidylinositol 3-kinase; PPAR, peroxisome proliferator-activated receptor; ROS, reactive oxygen species; SREBP, sterol-regulatory element binding protein; TBP, TATA binding protein.

ation in the host genome. The central dogma is defined as the flow of genetic information from DNA to mRNA and then to protein, so genetic/genomic alterations and transcriptional/translational modifications are ultimately considered to affect the cellular signaling pathway at the transcriptional level.

Over the past decade, several methods (including differential display, serial analysis of gene expression [SAGE], and microarray) have been developed to allow comparative studies of gene expression between normal and cancer cells on a genome-wide scale,[58] and the analysis of a set of all RNA molecules (mainly indicating mRNAs) is termed as whole transcriptome analysis. Extensive transcriptome analysis of HCC and corresponding noncancerous livers has been performed, and the results have greatly increased our knowledge about the transcriptome characteristics of HCV-related HCC.

Early microarray and SAGE studies investigating the gene expression patterns of chronic hepatitis B and C tissues indicated that these two chronic hepatitis tissues had distinct gene expression profiles; the genes activated in chronic hepatitis C were correlated with signaling pathways associated with apoptosis, oxidative stress responses, and Th1 cytokine signaling.[59,60] An early study comparing genes activated in HCV-related and HBV-related HCCs showed that the genes associated with xenobiotic metabolism were more abundantly expressed in HCV-related HCC,[61] suggesting a detoxification role, which is potentially induced by chronic inflammation and generation of ROS resulting from HCV infection. In contrast, HBV-related HCC might closely correlate with the activation of imprint genes, including insulin-like growth factor-II (IGF-II) as investigated by oligo-DNA microarray,[62] suggesting a role of de-differentiation or epigenetic alteration of the host genome in HBV-related HCC. Activation of genes associated with interferon, oxidative stress, apoptosis, and lipid metabolism signaling was detected in HCV-related HCC and chronic hepatitis C specimens,[27,60,63] consistent with numerous functional studies that have investigated the host response evoked by HCV structural and non-structural proteins.[48]

Transcriptome analysis has also recently shed new light on the transcriptional alteration events occurring in early stages of HCV-related hepatocarcinogenesis. *GPC3* (encoding Glypican 3) was identified as one of the most activated transcripts in the early stage of hepatocarcinogenesis,[60,64] while several recent studies showed that gene signatures including *GPC3* can successfully discriminate HCCs from pre-malignant dysplastic nodules and cirrhosis nodules.[65,66] Close examination of genes differentially expressed among cirrhotic nodules, dysplastic nodules, and early and advanced HCV-related HCC tissues has also suggested roles for Toll-like receptor signaling, Wnt signaling, bone morphogenetic protein (BMP)/TGF-β signaling, JAK-STAT signaling, and DNA repair/cell cycle responses in each step of the malignant transformation processes.[67] These processes might therefore provide candidate molecular targets for the chemoprevention of HCV-related HCC.

Recent advances in transcriptome analysis have also provided detailed information on the status of small noncoding RNAs, microRNAs, that can regulate the expression of target genes and viral replication in normal and cancer tissues. Expression of microRNAs including miR-122 and −199a has been reported to modulate HCV replication,[68–70] and miR-122 expression can be regulated by host interferon signaling and responses.[71] HCV protein expression in turn could induce miRNAs and might affect the tumor suppressor DLC1 and the chemosensitivity of malignantly transformed cells.[72,73] Several microRNAs were also differentially expressed between HCV-related and HBV-related HCCs as well as their corresponding non-cancerous liver tissues. The candidate signaling pathways potentially altered by microRNAs in HCV-related tissues were those associated with antigen presentation, cell cycle, and lipid metabolism,[74] consistent with the mRNA microarray data described above. MicroRNAs have also recently been reported to successfully discriminate between HCC and cirrhotic liver tissues,[75] implicating their role in the early stages of malignant transformation. These data suggest that microRNAs may be good targets for the eradication of HCC as well as hepatocytes infected with HCV.

Conclusion

The heterogeneity of genetic/transcriptomic/proteomic events observed in hepatocytes or cell lines expressing HCV proteins and HCV-related HCCs reported thus far has suggested that complex mechanisms underlie malignant transformation induced by HCV infection. These potentially act through convoluted virus-host interactions including HCV replication with host cell cycles, apoptosis, proliferation, quality control of protein synthesis, lipid metabolism, and DNA damage responses. Indeed, HCC is a heterogeneous disease in terms of drug sensitivity, metastatic capacity, and clinical outcome. The heterogeneity of HCV-related HCC may closely correlate with the origin of malignantly transformed cells where multifaceted cellular reactions including apoptosis and

cell proliferation are induced by HCV infection. An in-depth understanding of these molecular complexities associated with HCV-related HCC may provide the opportunity for effective chemoprevention of HCC among those with HCV-cirrhosis, and to design tailor-made treatment options for HCV-related HCC patients in the future.

References

1 Parkin DM, Bray F, Ferlay J, Pisani P. Global cancer statistics, 2002. *CA Cancer J. Clin.* 2005; **55**: 74–108.
2 Yang JD, Roberts LR. Hepatocellular carcinoma: a global view. *Nat. Rev. Gastroenterol. Hepatol.* 2010; **7**: 448–58.
3 Thomas DL, Thio CL, Martin MP *et al.* Genetic variation in IL28B and spontaneous clearance of hepatitis C virus. *Nature* 2009; **461**: 798–801.
4 Tillmann HL, Thompson AJ, Patel K *et al.* A polymorphism near IL28B is associated with spontaneous clearance of acute hepatitis C virus and jaundice. *Gastroenterology* 2010; **139**: 1586–92. 92 e1.
5 Bruix J, Barrera JM, Calvet X *et al.* Prevalence of antibodies to hepatitis C virus in Spanish patients with hepatocellular carcinoma and hepatic cirrhosis. *Lancet* 1989; **2**: 1004–6.
6 Colombo M, Kuo G, Choo QL *et al.* Prevalence of antibodies to hepatitis C virus in Italian patients with hepatocellular carcinoma. *Lancet* 1989; **2**: 1006–8.
7 Liang TJ, Heller T. Pathogenesis of hepatitis C-associated hepatocellular carcinoma. *Gastroenterology* 2004; **127**: S62–71.
8 Yoshizawa H. Hepatocellular carcinoma associated with hepatitis C virus infection in Japan: projection to other countries in the foreseeable future. *Oncology* 2002; **62** (Suppl. 1): 8–17.
9 Yuen MF, Hou JL, Chutaputti A. Hepatocellular carcinoma in the Asia pacific region. *J. Gastroenterol. Hepatol.* 2009; **24**: 346–53.
10 El-Serag HB, Rudolph KL. Hepatocellular carcinoma: epidemiology and molecular carcinogenesis. *Gastroenterology* 2007; **132**: 2557–76.
11 Fattovich G, Stroffolini T, Zagni I, Donato F. Hepatocellular carcinoma in cirrhosis: incidence and risk factors. *Gastroenterology* 2004; **127**: S35–50.
12 Yu MC, Yuan JM. Environmental factors and risk for hepatocellular carcinoma. *Gastroenterology* 2004; **127**: S72–8.
13 Kawaguchi T, Sata M. Importance of hepatitis C virus-associated insulin resistance: therapeutic strategies for insulin sensitization. *World J. Gastroenterol.* 2010; **16**: 1943–52.
14 Penin F, Dubuisson J, Rey FA, Moradpour D, Pawlotsky JM. Structural biology of hepatitis C virus. *Hepatology* 2004; **39**: 5–19.
15 Tsai WL, Chung RT. Viral hepatocarcinogenesis. *Oncogene* 2010; **29**: 2309–24.
16 Levrero M. Viral hepatitis and liver cancer: the case of hepatitis C. *Oncogene* 2006; **25**: 3834–47.
17 Akuta N, Suzuki F, Kawamura Y *et al.* Amino acid substitutions in the hepatitis C virus core region are the important predictor of hepatocarcinogenesis. *Hepatology* 2007; **46**: 1357–64.
18 Fishman SL, Factor SH, Balestrieri C *et al.* Mutations in the hepatitis C virus core gene are associated with advanced liver disease and hepatocellular carcinoma. *Clin. Cancer Res.* 2009; **15**: 3205–13.
19 Moriya K, Fujie H, Shintani Y *et al.* The core protein of hepatitis C virus induces hepatocellular carcinoma in transgenic mice. *Nat. Med.* 1998; **4**: 1065–7.
20 Okuda M, Li K, Beard MR *et al.* Mitochondrial injury, oxidative stress, and antioxidant gene expression are induced by hepatitis C virus core protein. *Gastroenterology* 2002; **122**: 366–75.
21 Perlemuter G, Sabile A, Letteron P *et al.* Hepatitis C virus core protein inhibits microsomal triglyceride transfer protein activity and very low density lipoprotein secretion: a model of viral-related steatosis. *FASEB J.* 2002; **16**: 185–94.
22 Kawamura T, Furusaka A, Koziel MJ *et al.* Transgenic expression of hepatitis C virus structural proteins in the mouse. *Hepatology* 1997; **25**: 1014–21.
23 Wakita T, Taya C, Katsume A *et al.* Efficient conditional transgene expression in hepatitis C virus cDNA transgenic mice mediated by the Cre/loxP system. *J. Biol. Chem.* 1998; **273**: 9001–6.
24 Lerat H, Kammoun HL, Hainault I *et al.* Hepatitis C virus proteins induce lipogenesis and defective triglyceride secretion in transgenic mice. *J. Biol. Chem.* 2009; **284**: 33466–74.
25 Ohata K, Hamasaki K, Toriyama K *et al.* Hepatic steatosis is a risk factor for hepatocellular carcinoma in patients with chronic hepatitis C virus infection. *Cancer* 2003; **97**: 3036–43.
26 Kurosaki M, Hosokawa T, Matsunaga K *et al.* Hepatic steatosis in chronic hepatitis C is a significant risk factor for developing hepatocellular carcinoma independent of age, sex, obesity, fibrosis stage and response to interferon therapy. *Hepatol. Res.* 2010; **40**: 870–7.
27 Yamashita T, Honda M, Takatori H *et al.* Activation of lipogenic pathway correlates with cell proliferation and poor prognosis in hepatocellular carcinoma. *J. Hepatol.* 2009; **50**: 100–10.
28 Dharancy S, Malapel M, Perlemuter G *et al.* Impaired expression of the peroxisome proliferator-activated receptor alpha during hepatitis C virus infection. *Gastroenterology* 2005; **128**: 334–42.
29 Waris G, Felmlee DJ, Negro F, Siddiqui A. Hepatitis C virus induces proteolytic cleavage of sterol regulatory element binding proteins and stimulates their phosphorylation via oxidative stress. *J. Virol.* 2007; **81**: 8122–30.
30 Tanaka N, Moriya K, Kiyosawa K, Koike K, Gonzalez FJ, Aoyama T. PPARalpha activation is essential for HCV core protein-induced hepatic steatosis and hepatocellular carcinoma in mice. *J. Clin. Invest.* 2008; **118**: 683–94.
31 Korenaga M, Wang T, Li Y *et al.* Hepatitis C virus core protein inhibits mitochondrial electron transport and increases reactive oxygen species (ROS) production. *J. Biol. Chem.* 2005; **280**: 37481–8.
32 Li Y, Boehning DF, Qian T, Popov VL, Weinman SA. Hepatitis C virus core protein increases mitochondrial ROS production by stimulation of Ca^{2+} uniporter activity. *FASEB J.* 2007; **21**: 2474–85.
33 Furutani T, Hino K, Okuda M *et al.* Hepatic iron overload induces hepatocellular carcinoma in transgenic mice expressing the hepatitis C virus polyprotein. *Gastroenterology* 2006; **130**: 2087–98.
34 Alisi A, Giambartolomei S, Cupelli F *et al.* Physical and functional interaction between HCV core protein and the different p73 isoforms. *Oncogene* 2003; **22**: 2573–80.
35 Honda M, Kaneko S, Shimazaki T *et al.* Hepatitis C virus core protein induces apoptosis and impairs cell-cycle regulation in stably transformed Chinese hamster ovary cells. *Hepatology* 2000; **31**: 1351–9.
36 Kao CF, Chen SY, Chen JY, Lee YHW. Modulation of p53 transcription regulatory activity and post-translational modification by hepatitis C virus core protein. *Oncogene* 2004; **23**: 2472–83.
37 Otsuka M, Kato N, Lan K *et al.* Hepatitis C virus core protein enhances p53 function through augmentation of DNA binding affinity and transcriptional ability. *J. Biol. Chem.* 2000; **275**: 34122–30.
38 Ray RB, Steele R, Meyer K, Ray R. Hepatitis C virus core protein represses p21WAF1/Cip1/Sid1 promoter activity. *Gene* 1998; **208**: 331–6.
39 Yamanaka T, Kodama T, Doi T. Subcellular localization of HCV core protein regulates its ability for p53 activation and p21 suppression. *Biochem. Biophys. Res. Commun.* 2002; **294**: 528–34.

40 Lee SK, Park SO, Joe CO, Kim YS. Interaction of HCV core protein with 14-3-3epsilon protein releases Bax to activate apoptosis. *Biochem. Biophys. Res. Commun.* 2007; **352**: 756–62.
41 Mohd-Ismail NK, Deng L, Sukumaran SK, Yu VC, Hotta H, Tan YJ. The hepatitis C virus core protein contains a BH3 domain that regulates apoptosis through specific interaction with human Mcl-1. *J. Virol.* 2009; **83**: 9993–10006.
42 Saito K, Meyer K, Warner R, Basu A, Ray RB, Ray R. Hepatitis C virus core protein inhibits tumor necrosis factor alpha-mediated apoptosis by a protective effect involving cellular FLICE inhibitory protein. *J. Virol.* 2006; **80**: 4372–9.
43 Tsutsumi T, Suzuki T, Moriya K *et al.* Hepatitis C virus core protein activates ERK and p38 MAPK in cooperation with ethanol in transgenic mice. *Hepatology* 2003; **38**: 820–8.
44 Matsuzaki K, Murata M, Yoshida K *et al.* Chronic inflammation associated with hepatitis C virus infection perturbs hepatic transforming growth factor beta signaling, promoting cirrhosis and hepatocellular carcinoma. *Hepatology* 2007; **46**: 48–57.
45 Wang XW, Hussain SP, Huo TI *et al.* Molecular pathogenesis of human hepatocellular carcinoma. *Toxicology* 2002; **181–182**: 43–7.
46 Tanji Y, Kaneko T, Satoh S, Shimotohno K. Phosphorylation of hepatitis C virus-encoded nonstructural protein NS5A. *J. Virol.* 1995; **69**: 3980–6.
47 De Mitri MS, Cassini R, Bagaglio S *et al.* Evolution of hepatitis C virus non-structural 5A gene in the progression of liver disease to hepatocellular carcinoma. *Liver Int.* 2007; **27**: 1126–33.
48 Kasprzak A, Adamek A. Role of hepatitis C virus proteins (C, NS3, NS5A) in hepatic oncogenesis. *Hepatol. Res.* 2008; **38**: 1–26.
49 Benga WJ, Krieger SE, Dimitrova M *et al.* Apolipoprotein E interacts with hepatitis C virus nonstructural protein 5A and determines assembly of infectious particles. *Hepatology* 2010; **51**: 43–53.
50 Kim K, Kim KH, Ha E, Park JY, Sakamoto N, Cheong J. Hepatitis C virus NS5A protein increases hepatic lipid accumulation via induction of activation and expression of PPARgamma. *FEBS Lett.* 2009; **583**: 2720–6.
51 Kato N, Lan KH, Ono-Nita SK, Shiratori Y, Omata M. Hepatitis C virus nonstructural region 5A protein is a potent transcriptional activator. *J. Virol.* 1997; **71**: 8856–9.
52 Lan KH, Sheu ML, Hwang SJ *et al.* HCV NS5A interacts with p53 and inhibits p53-mediated apoptosis. *Oncogene* 2002; **21**: 4801–11.
53 Majumder M, Ghosh AK, Steele R, Ray R, Ray RB. Hepatitis C virus NS5A physically associates with p53 and regulates p21/waf1 gene expression in a p53-dependent manner. *J. Virol.* 2001; **75**: 1401–7.
54 Chung YL, Sheu ML, Yen SH. Hepatitis C virus NS5A as a potential viral Bcl-2 homologue interacts with Bax and inhibits apoptosis in hepatocellular carcinoma. *Int. J. Cancer* 2003; **107**: 65–73.
55 He Y, Nakao H, Tan SL *et al.* Subversion of cell signaling pathways by hepatitis C virus nonstructural 5A protein via interaction with Grb2 and P85 phosphatidylinositol 3-kinase. *J. Virol.* 2002; **76**: 9207–17.
56 Park CY, Choi SH, Kang SM *et al.* Nonstructural 5A protein activates beta-catenin signaling cascades: implication of hepatitis C virus-induced liver pathogenesis. *J. Hepatol.* 2009; **51**: 853–64.
57 Peng L, Liang D, Tong W, Li J, Yuan Z. Hepatitis C virus NS5A activates the mammalian target of rapamycin (mTOR) pathway, contributing to cell survival by disrupting the interaction between FK506-binding protein 38 (FKBP38) and mTOR. *J. Biol. Chem.* 2010; **285**: 20870–81.
58 Yamashita T, Honda M, Kaneko S. Application of serial analysis of gene expression in cancer research. *Curr. Pharm. Biotechnol.* 2008; **9**: 375–82.
59 Honda M, Kaneko S, Kawai H, Shirota Y, Kobayashi K. Differential gene expression between chronic hepatitis B and C hepatic lesion. *Gastroenterology* 2001; **120**: 955–66.
60 Yamashita T, Kaneko S, Hashimoto S *et al.* Serial analysis of gene expression in chronic hepatitis C and hepatocellular carcinoma. *Biochem. Biophys. Res. Commun.* 2001; **282**: 647–54.
61 Okabe H, Satoh S, Kato T *et al.* Genome-wide analysis of gene expression in human hepatocellular carcinomas using cDNA microarray: identification of genes involved in viral carcinogenesis and tumor progression. *Cancer Res.* 2001; **61**: 2129–37.
62 Iizuka N, Oka M, Yamada-Okabe H *et al.* Comparison of gene expression profiles between hepatitis B virus- and hepatitis C virus-infected hepatocellular carcinoma by oligonucleotide microarray data on the basis of a supervised learning method. *Cancer Res.* 2002; **62**: 3939–44.
63 Honda M, Yamashita T, Ueda T, Takatori H, Nishino R, Kaneko S. Different signaling pathways in the livers of patients with chronic hepatitis B or chronic hepatitis C. *Hepatology* 2006; **44**: 1122–38.
64 Capurro M, Wanless IR, Sherman M *et al.* Glypican-3: a novel serum and histochemical marker for hepatocellular carcinoma. *Gastroenterology* 2003; **125**: 89–97.
65 Jia HL, Ye QH, Qin LX *et al.* Gene expression profiling reveals potential biomarkers of human hepatocellular carcinoma. *Clin. Cancer Res.* 2007; **13**: 1133–9.
66 Llovet JM, Chen Y, Wurmbach E *et al.* A molecular signature to discriminate dysplastic nodules from early hepatocellular carcinoma in HCV cirrhosis. *Gastroenterology* 2006; **131**: 1758–67.
67 Wurmbach E, Chen YB, Khitrov G *et al.* Genome-wide molecular profiles of HCV-induced dysplasia and hepatocellular carcinoma. *Hepatology* 2007; **45**: 938–47.
68 Jopling CL, Yi M, Lancaster AM, Lemon SM, Sarnow P. Modulation of hepatitis C virus RNA abundance by a liver-specific MicroRNA. *Science* 2005; **309**: 1577–81.
69 Murakami Y, Aly HH, Tajima A, Inoue I, Shimotohno K. Regulation of the hepatitis C virus genome replication by miR-199a. *J. Hepatol.* 2009; **50**: 453–60.
70 Sarasin-Filipowicz M, Krol J, Markiewicz I, Heim MH, Filipowicz W. Decreased levels of microRNA miR-122 in individuals with hepatitis C responding poorly to interferon therapy. *Nat. Med.* 2009; **15**: 31–3.
71 Pedersen IM, Cheng G, Wieland S *et al.* Interferon modulation of cellular microRNAs as an antiviral mechanism. *Nature* 2007; **449**: 919–22.
72 Braconi C, Valeri N, Gasparini P *et al.* Hepatitis C virus proteins modulate microRNA expression and chemosensitivity in malignant hepatocytes. *Clin. Cancer Res.* 2010; **16**: 957–66.
73 Banaudha K, Kaliszewski M, Korolnek T *et al.* MicroRNA silencing of tumor suppressor DLC-1 promotes efficient hepatitis C virus replication in primary human hepatocytes. *Hepatology* 2011; **53**: 53–61.
74 Ura S, Honda M, Yamashita T *et al.* Differential microRNA expression between hepatitis B and hepatitis C leading disease progression to hepatocellular carcinoma. *Hepatology* 2009; **49**: 1098–112.
75 Wong QW, Lung RW, Law PT *et al.* MicroRNA-223 is commonly repressed in hepatocellular carcinoma and potentiates expression of Stathmin1. *Gastroenterology* 2008; **135**: 257–69.

UICC
global cancer control

IJC
International Journal of Cancer

Identification of a secretory protein c19orf10 activated in hepatocellular carcinoma

Hajime Sunagozaka, Masao Honda, Taro Yamashita, Ryuhei Nishino, Hajime Takatori, Kuniaki Arai, Tatsuya Yamashita, Yoshio Sakai and Shuichi Kaneko

Department of Gastroenterology, Kanazawa University Hospital, Kanazawa, Ishikawa, Japan

The identification of genes involved in tumor growth is crucial for the development of inventive anticancer treatments. Here, we have cloned a 17-kDa secretory protein encoded by *c19orf10* from hepatocellular carcinoma (HCC) serial analysis of gene expression libraries. Gene expression analysis indicated that *c19orf10* was overexpressed in approximately two-thirds of HCC tissues compared to the adjacent noncancerous liver tissues, and its expression was significantly positively correlated with that of alpha-fetoprotein (AFP). Overexpression of *c19orf10* enhanced cell proliferation of AFP-negative HLE cells, whereas knockdown of *c19orf10* inhibited cell proliferation of AFP-positive Hep3B and HuH7 cells along with G1 cell cycle arrest. Supplementation of recombinant c19orf10 protein in culture media enhanced cell proliferation in HLE cells, and this effect was abolished by the addition of antibodies developed against c19orf10. Intriguingly, c19orf10 could regulate cell proliferation through the activation of Akt/mitogen-activated protein kinase pathways. Taken together, these data suggest that c19orf10 might be one of the growth factors and potential molecular targets activated in HCC.

Hepatocellular carcinoma (HCC) is one of the most common cancers with an estimated worldwide incidence of 1,000,000 cases per year.[1] Most HCCs develop as a consequence of chronic liver disease such as chronic viral hepatitis due to hepatitis C virus (HCV) or hepatitis B virus (HBV) infection.[2–7] Liver cirrhosis patients with any etiology are considered to be at an extremely high risk for HCC.[8–10] Indeed, ~7% of liver cirrhosis patients with HCV infection develop HCC annually,[8,11] and the advancement of reliable HCC screening methods for high-risk patients is crucial for the improvement of their overall survival.[12]

Currently, imaging diagnostic techniques such as ultrasonography, computed tomography, magnetic resonance image and angiography are the gold standards for the early detection of HCC.[13,14] In addition, tumor markers such as alpha-fetoprotein (AFP) and des-gamma carboxyl prothrombin (DCP) have been used for the screening of HCC,[15–18] although their sensitivity and specificity are not sufficiently high. Recently, a gene expression profiling approach shed new light on Glypican 3, a heparin sulfate proteoglycan anchored to the plasma membrane, as a potential HCC marker, and its clinical usefulness as a molecular target as well as a tumor marker is presently under investigation.[19]

There are several options available for the treatment of HCC, including surgical resection, liver transplantation, radiofrequency ablation, transcatheter arterial chemoembolization and chemotherapy, while taking the HCC stage and liver function into consideration. Recently, molecular therapy targeting the Raf kinase/vascular endothelial growth factor receptor (VEGFR) kinase inhibitor sorafenib improved the survival of patients with advanced HCC,[20,21] emphasizing the importance of deciphering the molecular pathogenesis of HCC for the development of effective treatment options.

Here, we investigated the gene expression profiles of HCC by serial analysis of gene expression (SAGE) to discover a novel gene activated in HCC.[22–25] We identified a gene, *c19orf10*, overexpressed in HCC and determined that the encoded 17-kDa protein (c19orf10) is a secretory protein. Murine *c19orf10* was originally discovered to encode a cytokine interleukin (IL)-25/stroma-derived growth factor (SF20) in 2001.[26] The gene *c19orf10* was mapped in the H2 complex region of mouse chromosome 17 between *C3* and *Ir5*, and the hypothetical protein was predicted as globular protein.[26] However, the subsequent study failed to reproduce its proliferative effect on lymphoid cells, and the paper was retracted by the authors in 2003.[26,27] Nevertheless, independent studies revealed that c19orf10 was indeed produced by synoviocytes, macrophages and adipocytes, although the function of c19orf10 remained elusive.[28,29] In our study, we identified that *c19orf10* was overexpressed in AFP-positive HCC samples. Our data imply that c19orf10 could activate the mitogen-activated protein kinase (MAPK)/Akt pathway and

Key words: hepatocellular carcinoma, serial analysis of gene expression, *c19orf10*
Additional Supporting Information may be found in the online version of this article
DOI: 10.1002/ijc.25830
History: Received 14 Mar 2010; Accepted 15 Nov 2010; Online 2 Dec 2010
Correspondence to: Shuichi Kaneko, Kanazawa University Hospital, 13-1 Takara-machi, Kanazawa, Ishikawa 920-8641, Japan,
Tel.: +81-76-265-2233, Fax: +81-76-234-4250,
E-mail: skaneko@m-kanazawa.jp

enhance cell proliferation in HCC cell lines, suggesting that c19orf10 may be a growth factor produced by tumor epithelial cells and/or stromal cells, and, therefore, would be a good target for the treatment of HCC.

Material and Methods

SAGE and HCC samples

HCC and normal liver SAGE libraries that we had constructed were reanalyzed using SAGE 2000 software. The size of each SAGE library was normalized to 300,000 transcripts per library. Monte Carlo simulation was used to select genes whose expression levels were significantly different between the two libraries. Each SAGE tag was annotated using the gene-mapping website SAGE Genie database (http://cgap.nci.nih.gov/SAGE/) and the SOURCE database (http://smd.stanford.edu/cgi-bin/source/sourceSearch) as previously described.[30] An additional 15 SAGE libraries of normal and cancerous tissues from various organs were retrieved using the National Center for Biotechnology Information SAGEmap (http://www.ncbi.nlm.nih.gov/SAGE/).

Fifteen HCC tissues (four HBV-related and 11 HCV-related) and the corresponding noncancerous liver tissues were obtained from HCC patients who received hepatectomy. Four normal liver tissues were obtained from patients undergoing surgical resection of the liver for the treatment of metastatic colon cancer. Additionally, 36 HCC tissues (17 HBV-related and 19 HCV-related) were obtained from HCC patients undergoing hepatectomy. These samples were snap frozen in liquid nitrogen immediately after resection and used for quantitative real-time detection PCR (RTD-PCR). Total RNA was extracted using a ToTALLY RNA™ kit (Ambion, Austin, TX).

The study protocol conformed to the ethical guidelines of the Declaration of Helsinki (1975) and was approved by the institutional ethical review board committee. All patients provided written informed consent for the analysis of the specimens.

Laser capture microdissection and RNA isolation

Laser capture microdissection (LCM) was performed as previously described.[31] Briefly, 20 HCV-related surgically resected HCC tissues were frozen in OCT compound (Sakura Finetech, Torrance, CA).[32] Inflammatory cells and cancerous cells in HCC tissues were separately excised by LCM using a Laser Scissors CRI-337 (Cell Robotics, Albuquerque, NM) under a microscope. Total RNA was isolated from these cells using a microRNA isolation kit (Stratagene, La Jolla, CA) in accordance with the supplied protocol, with slight modifications.[31]

Construction of C19ORF10 expression plasmid and recombinant adenovirus vector

PCR was performed on a Marathon cDNA library from Huh7 cells using the following primers: sense primers: 5′-GACCCTAGTCCAACATGGCGGCGCCC-3′ (the first PCR), 5′-ATGGCGGCGCCCAGCGGAGGGTGGAACGGC-3′ (the nested second PCR) and antisense primers: 5′-CACCGGA GATGAGAAGGTGCCACCCGC-3′ (the first PCR), 5′-CAG GGCTGCTGGTCACAGCTCAGTGCGCG-3′ (the nested second PCR). The 5′ and 3′ends of the cDNA were isolated using a SMART RACE cDNA Amplification kit (Clontech, Mountain View, CA) according to the manufacturer's recommendations. The PCR products were cloned into a TA vector (Invitrogen, Carlsbad, CA) to generate the pcDNA3.1-*c19orf10* expression plasmid. Using this plasmid, a C-terminally FLAG-tagged construct of *c19orf10* was generated and inserted in a pSI mammalian expression vector (Promega, Madison, WI), which was driven by the SV40 promoter (pSI-*c19orf10*).

The replication-incompetent recombinant adenovirus vector expressing FLAG-tagged *c19orf10* (Ad. *c19orf10-FLAG*) was generated by homologous recombination using the AdMax system (Microbix, Toronto, Canada) as previously described.[33] The generated recombinant adenovirus was purified by limiting dilution, and the titer of viral aliquots was determined by the 50% tissue culture infectious dose method as previously described.[34]

RTD-PCR

RTD-PCR was performed as previously described.[31] Briefly, template cDNA was synthesized from 1 μg of total RNA using SuperScript™ II RT (Invitrogen). RTD-PCR of *c19orf10* (Hs. 00384077_m1), *AFP* (Hs00173490_m1), *GPC3* (Hs01018938_m1), *KRT19* (Hs00761767_s1) and the *ACTB* internal control (Hs99999903_m1) was performed using a TaqMan® Gene Expression Assay kit (Applied Biosystems, Foster City, CA). The expression of selected genes was measured in triplicate by ΔΔCT method using the 7900 Sequence Detection System (Applied Biosystems).

Cell lines and transfection of plasmids

Human liver cancer cell lines HuH1, Huh7, Hep3B, HLE and HLF as well as HEK293 and NIH3T3 were cultured in Dulbecco's modified Eagle's medium (Invitrogen) supplemented with 10% heat-inactivated fetal bovine serum (Invitrogen) in 5% CO_2 at 37°C. Transfection of plasmids was performed using FuGENE™ 6 (Roche Diagnostics, Indianapolis, IN) according to the manufacturer's instruction. Briefly, 5×10^5 cells were seeded in a six-well plate 12 hr before transfection, and 3 μg of plasmid DNA was used for each transfection. All experiments were repeated at least twice.

Purification of c19orf10-FLAG fused protein and production of anti-c19orf10 antibody

Approximately 500 ml of culture supernatant obtained from HEK293 cells infected with Ad. *C19ORF10-FLAG* at a multiplicity of infection of 20 was applied to an anti-FLAG affinity gel column (Sigma-Aldrich, St. Louis, MO). The column was

Table 1. ESTs overexpressed in the HCC library

Tag sequence	*p* value	HCC	Normal liver	T/N ratio	Name	UniGene ID
TGGGCAGGTG	<0.00001	33	0	>33	Chromosome 5 open reading frame 13	Hs.483067
GCAAAATATC	<0.00001	31	2	15.5	Liver cancer-associated noncoding mRNA, partial sequence	Hs.214343
AGCCTGCAGA	0.0002	12	1	12	Chromosome 19 open reading frame 10	Hs.465645
TTGTGCACGT	0.000228	12	1	12	CDNA FLJ45284 fis, clone BRHIP3001964	Hs.514273
ACATTCTTGT	0.000042	12	0	>12	Transcribed locus, strongly similar to XP_496055.1	Hs.76704
ACAAGTACCC	0.001161	10	1	>10	Chromosome 5 open reading frame 13	Hs.483067
GAGGTGAAGG	0.000174	10	0	>10	KIAA1914	Hs.501106
GCTGGAGGAG	0.000114	10	0	>10	Transcribed locus	Hs.520115

subjected to elution by competition with FLAG peptide (5 μg/ml), and each 1 ml fraction of the eluted aliquot was collected to obtain the most concentrated c19orf10-FLAG protein in accordance with the manufacturer's protocol. The anti-c19orf10 antibodies were developed by immunizing rabbits with repeated intradermal injections of purified c19orf10-FLAG. Protein concentration was measured by the Bradford method.

Silencing gene expression by short interfering RNA

The selected short interfering RNA (siRNA) targeting *C19ORF10* (Si-*C19ORF10*; Silencer Select siRNAs s31855) and the irrelevant control sequence (Si-*Control*; Silencer Select siRNAs 4390843) was obtained from Applied Biosystems. Transfection of these siRNAs was performed using FuGENE^{TM} 6 (Roche Diagnostics) as previously described.[30] Briefly, 2×10^5 cells were seeded in a six-well plate 12 hr before transfection. A total of 100 pmol/l of siRNA duplex was used for each transfection. The experiments were performed at least twice.

Cell proliferation assay

Cell proliferation was evaluated in quadruplicate using a Cell Titer 96 MTS Assay kit (Promega). Briefly, 2×10^3 HLE or HuH7 cells were harvested in a 96-well plate 12 hr before the transfection or addition of the recombinant proteins. Transfection of siRNAs or plasmids was performed using FuGENE^{TM} 6 (Roche Diagnostics). After incubation with MTS/PMS solution at 37°C for 2 hr, the absorbance at 450 nm was measured. The experiments were performed at least twice.

Cell cycle analysis

Cells were fixed using 80% ice-cold ethanol and incubated with propidium iodide for 10 min. DNA content was analyzed using a FACS Caliber flow cytometer (BD Biosciences, San Jose, CA) counting 10,000 stained cells. The distribution of cells in each cell cycle phase was determined using FlowJo software (Tree Star, Ashland, OR).

Western blotting

Cells were lysed in radioimmunoprecipitation assay (RIPA) buffer, and the extracts were subsequently electrophoresed on sodium dodecyl sulfate–10% polyacrylamide gels and transferred onto protean nitrocellulose membranes. The blots were then incubated for 1 hr with an appropriate primary monoclonal antibody: phospho-PI3K (#4228), phospho-Akt (#4060), phospho-GSK-3β (#9323), phospho-c-Raf (#9427), phospho-MEK1/2 (#9154), phospho-p44/42 MAPK (Erk1/2) (#4370), Cdk4 (CDK4 (#2906)), Cdk6 (#3136), cyclinD1 (#2926), cyclinD3 (#2936), phospho-Rb (#9308), phospho-P53 (# 9286), phospho-cdc2 (#9111) and β-actin (#4970) (Cell Signaling Technology, Allschwil, Switzerland) and anti-FLAG antibodies (Sigma-Aldrich, St. Louis, MO). The blots were washed and exposed to peroxidase-conjugated secondary antibodies, such as anti-mouse or rabbit IgG antibodies, and visualized using the ECL^{TM} kit (Amersham Biosciences, Piscataway, NJ). All experiments were performed at least twice.

Statistical analyses

Unpaired *t*-tests and Kruskal–Wallis tests were performed on the RTD-PCR and cell proliferation data using GraphPad Prism software (www.graphpad.com).

Results

Identification of *C19ORF10* overexpression in HCC by SAGE

To comprehensively explore the candidate novel genes activated in HCC, we reanalyzed two SAGE libraries derived from HCC tissues and normal liver tissues.[30] After normalization of each SAGE library size to 300,000 tags, we compared the HCC and normal liver libraries to obtain the list of genes overexpressed in HCC. We identified 79 genes significantly overexpressed in the HCC library by more than tenfold when compared to the normal liver library (Supporting Information Table 1). Among them, we explored expressed sequence tags (ESTs) as candidates for novel HCC-related genes to identify eight unique tags corresponding to seven ESTs (Table 1). We especially focused on the EST chromosome 19 open reading frame 10 (*c19orf10*) because the

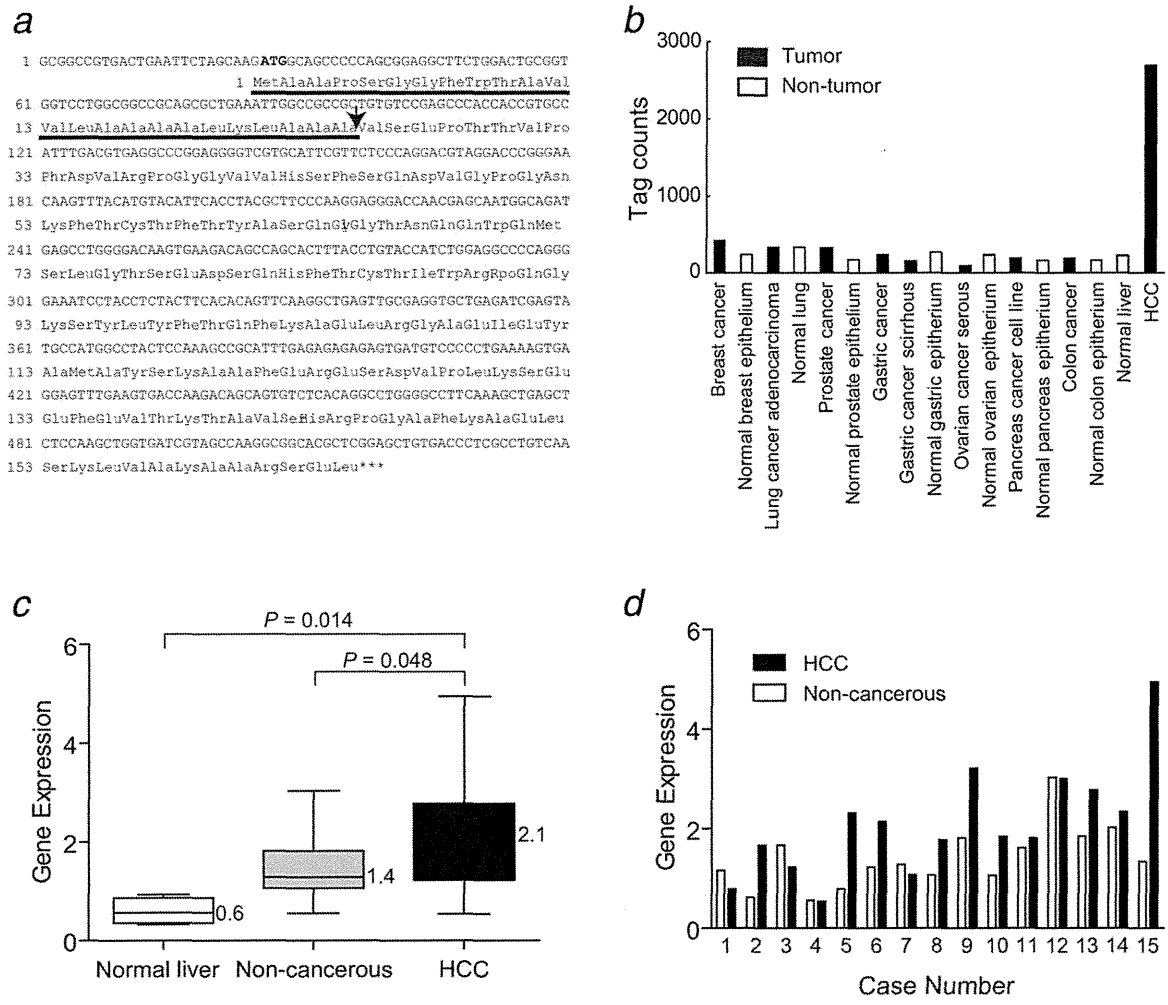

Figure 1. (*a*) Structure of a *c19orf10* gene and a c19orf10 protein. The DNA sequence of *c19orf10* and amino acid alignment of the encoded c19orf10 protein are shown. C19orf10 is predicted to have a molecular weight of 17 kDa and contain a signal peptide cleavage site (indicated as a black arrow). (*b*) *C19orf10* gene expression profiles in various tissues by SAGE. *Y*-axis indicates the number of tags corresponding to *c19orf10* in each tissue. (*c*, *d*) RTD-PCR analysis of *c19orf10*. RNA was isolated from 34 tissue samples: 15 HCC, 15 corresponding noncancerous liver samples and four normal liver samples. Differential expression of each gene among normal liver tissues, noncancerous liver tissues and HCC tissues was examined using the Kruskal–Wallis test and unpaired *t*-test. The mean value of gene expression data in each group is indicated (*c*). *C19orf10* was overexpressed in 10 of 15 examined HCC tissues compared to the noncancerous liver tissues (*d*).

sequence presumably encoded a secretory protein with a signal peptide sequence (Fig. 1*a*).

When we examined the expression profiles of *c19orf10* using retrieved SAGE data from various cancers and their normal counterparts, we identified that *c19orf10* was abundantly expressed in human HCC (Fig. 1*b*). We further examined the publicly available EST profiles of *c19orf10* (http://www.ncbi.nlm.nih.gov/unigene) and confirmed its tendency to be overexpressed in HCC compared to the normal liver (data not shown). We validated the overexpression of *c19orf10* in 15 independent HCC tissues and adjacent noncancerous liver tissues by RTD-PCR. Gene expression of *c19orf10* was significantly higher in the HCC tissues than in the normal liver tissues and adjacent noncancerous liver tissues ($p = 0.014$ and 0.048, respectively; Fig. 1*c*). *C19orf10* expression was elevated in HCC tissues compared to the adjacent noncancerous liver tissues in 10 of 15 patients (66.7%; Fig. 1*d*).

Overexpression of *C19ORF10* in AFP-positive HCC

As HCC is a heterogeneous mixture of cancer epithelial cells and stromal cells, and a previous report indicated that *c19orf10* is expressed in fibroblast-like synoviocytes. We, therefore, evaluated the expression of *c19orf10* in tumor epithelial cells and stromal cells separately using LCM and RTD-PCR in 20 HCC tissues (Fig. 2*a*). Although tumor

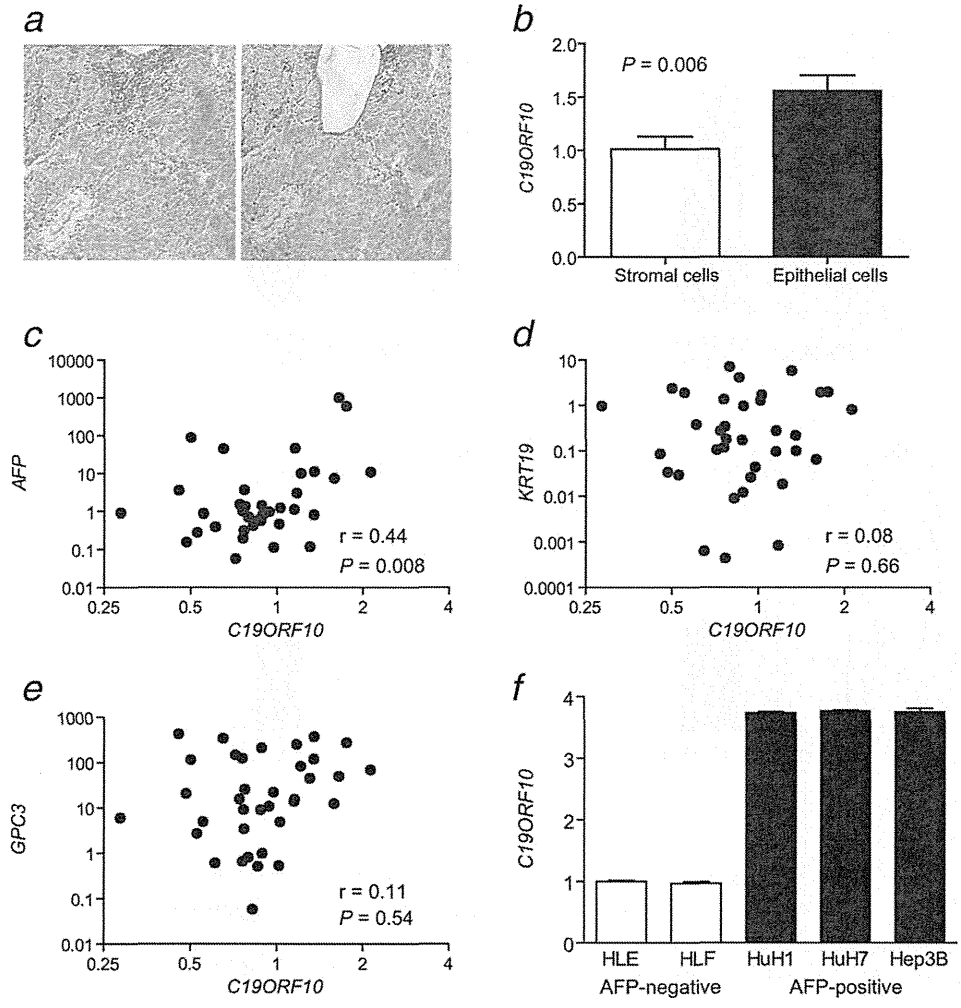

Figure 2. (*a*) Representative photomicrographs of an HCC tissue used for LCM (toluidine blue staining). Inflammatory mononuclear cells and stromal cells were separately captured (left: Pre-LCM, right: Post-LCM). (*b*) RTD-PCR analysis of *c19orf10* expression in inflammatory mononuclear cells and tumor epithelial cells in 20 HCV-related HCC tissues. Tumor-inflammatory mononuclear cells and stromal cells were isolated using LCM. RNAs were isolated from these cells as well as parenchymal tissues from the same liver, followed by RTD-PCR for *c19orf10* gene expression. Expression of the *c19orf10* gene was higher than that observed in HCC-infiltrating inflammatory mononuclear cells. *$p < 0.05$. (*c–e*) Scatter plot analysis of *c19orf10, AFP, KRT19* and *GPC3* expression in HCC. RNA was isolated from 17 HBV-related HCC and 19 HCV-related HCC. (*f*) RTD-PCR analysis of *c19orf10* in AFP-negative (HLE and HLF) and -positive (HuH1, HuH7 and Hep3B) liver cancer cell lines.

stromal cells expressed *c19orf10* at some level, the expression levels were significantly higher in tumor epithelial cells than in stromal cells ($p = 0.006$) (Fig. 2*b*).

To explore the relationship of *c19orf10* with other established HCC markers, we investigated the gene expression of *c19orf10*, *AFP* (alpha-fetoprotein), *KRT19* (cytokeratin 19) and *GPC3* (glypican 3). Because only 1 of 15 HCC tissues analyzed above (Fig. 1*d*) was AFP positive (data not shown), we further investigated the expression of *c19orf10* in an additional 36 HCC tissues using RTD-PCR. Interestingly, *c19orf10* expression was significantly positively correlated with *AFP* ($r = 0.44$, $p = 0.008$), but not with *KRT19* ($r = 0.08$, $p = 0.66$) nor *GPC3* ($r = 0.11$, $p = 0.54$) (Figs. 2*c–2e*). Furthermore, when we examined the expression of *c19orf10* in AFP-positive (HuH1, HuH7 and Hep3B) and -negative (HLE and HLF) HCC cell lines, we identified the overexpression of *c19orf10* in AFP-positive HCC cell lines (Fig. 2*f*). These data suggested that *c19orf10* is overexpressed and may play some role in AFP-positive HCCs.

C19orf10 regulates MAPK/Akt pathways and activates cell proliferation

To explore the functional role of c19orf10 in HCC, we performed *c19orf10* overexpression and knockdown studies using *c19orf10*-low HLE cells and *c19orf10*-high Hep3B and HuH7 cells, respectively. When we transfected HLE cells with

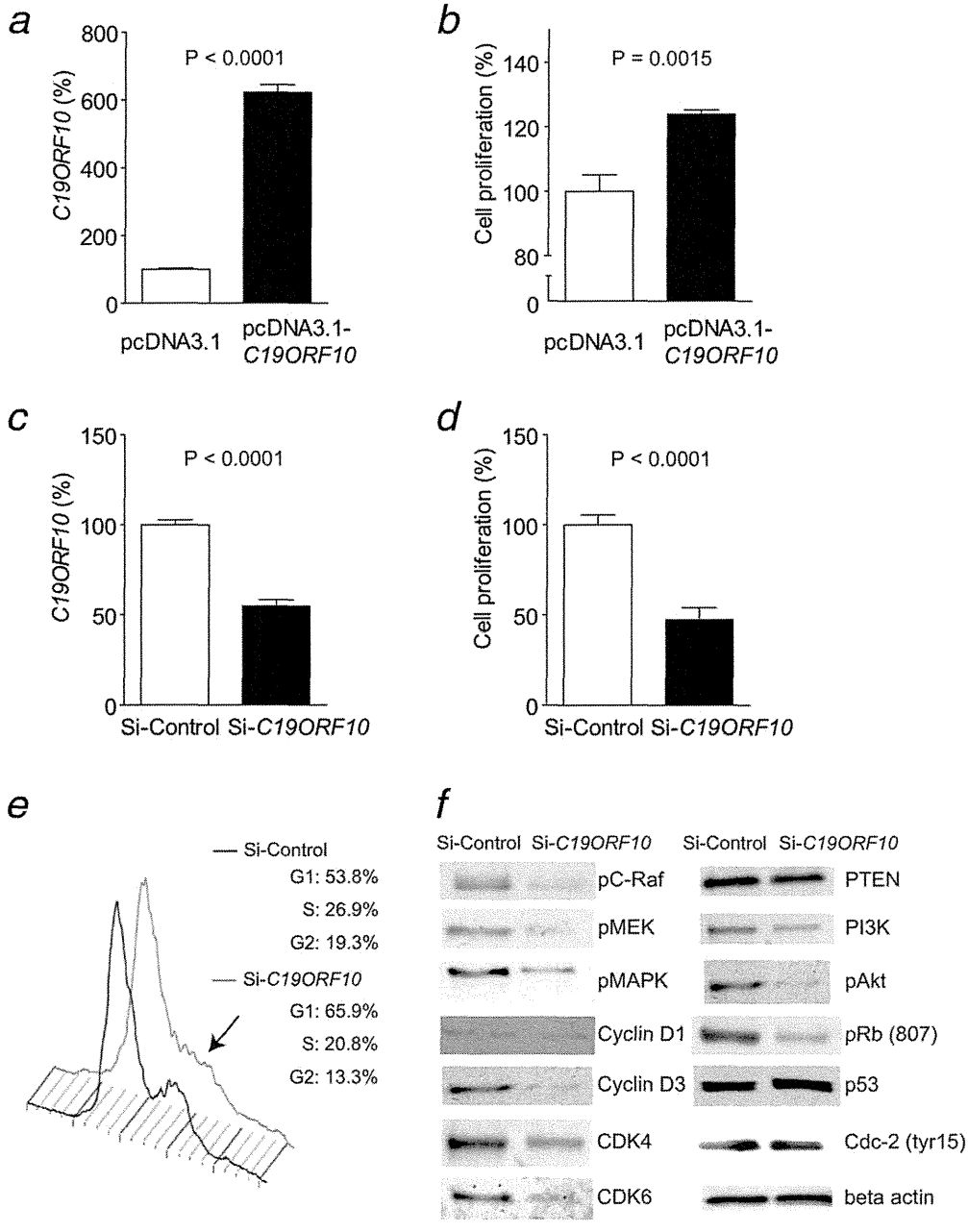

Figure 3. (*a*) RTD-PCR analysis of *c19orf10* expression in HLE cells transfected with pcDNA3.1 or pcDNA3.1-*c19orf10* plasmids. (*b*) Cell proliferation assay of HLE cells transfected with pcDNA3.1 or pcDNA3.1-*c19orf10* plasmids. Cell proliferation was evaluated 72 hr after each plasmid transfection. (*c*) RTD-PCR analysis of *c19orf10* expression in Hep3B cells transfected with Si-*Control* or Si-*c19orf10*. Gene expression was measured in triplicates 48 hr after transfection. (*d*) Cell proliferation assay of Hep3B cells transfected with Si-*Control* or Si-*c19orf10*. Cell proliferation was evaluated 72 hr after siRNA transfection. (*e*) Cell cycle analysis of HuH7 cells transfected with Si-*Control* or Si-*c19orf10*. Cell cycle was evaluated 72 hr after siRNA transfection. A black arrow indicates the G2 phase peak. (*f*) Western blotting analysis of Huh7 cells transfected with Si-*Control* or Si-*c19orf10*. Cells were lysed by RIPA buffer 72 hr after siRNA transfection.

pcDNA3.1 or pcDNA3.1-*c19orf10* plasmids, we identified an approximately sixfold overexpression of *c19orf10* when compared to the control 48 hr after transfection ($p < 0.0001$) (Fig. 3*a*). Interestingly, cell proliferation was modestly, but significantly, enhanced compared to the control 72 hr after transfection ($p = 0.0015$) (Fig. 3*b*).

We also transfected siRNAs targeting an irrelevant sequence (Si-*Control*) or *c19orf10* (Si-*c19orf10*) in Hep3B and

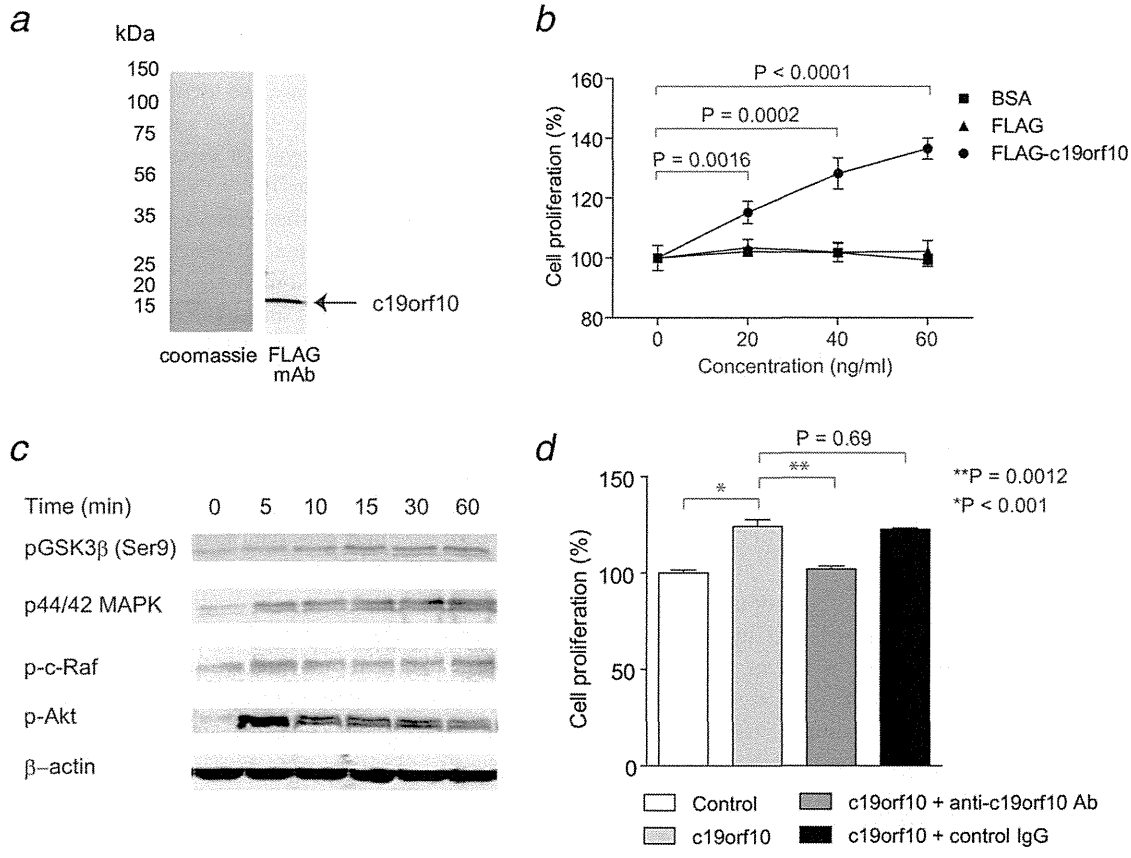

Figure 4. (*a*) Coomassie blue staining and Western blotting of culture supernatant of NIH3T3 cells transfected with pSI-*c19orf10-FLAG*. A black arrow indicates the 17-kDa c19orf10 protein. (*b*) Cell proliferation assay of HLE cells supplemented with recombinant c19orf10-FLAG, FLAG peptides or BSA. Cell proliferation was measured in quadruplicates 72 hr after supplementation. (*c*) Western blotting of HLE cells supplemented with c19orf10-FLAG (40 ng/ml). Cells were lysed at indicated time after c19orf10 supplementation. (*d*) Cell proliferation assay of HLE cells supplemented with control BSA (40 ng/ml) (white bar), c19orf10-FLAG (40 ng/ml) (light gray bar), c19orf10-FLAG (40 ng/ml) + anti-c19orf10 antibodies (gray bar) and c19orf10-FLAG (40 ng/ml) + control mouse IgG (black bar).

HuH7 cells. We observed an ~50% decrease in *c19orf10* expression in Hep3B cells transfected with Si- *c19orf10* compared to the control 48 hr after transfection with statistical significance ($p < 0.0001$). In this condition, cell proliferation was suppressed to 50% compared to the control 72 hr after transfection ($p < 0.0001$) (Figs. 3*c* and 3*d*). When we performed cell cycle analysis of HuH7 cells transfected with Si-*Control* or Si-*c19orf10*, we identified an increase of G1-phase cells and a decrease of S- and G2-phase cells by *c19orf10* knockdown, suggesting that the G1 cycle arrest was caused by the knockdown of *c19orf10* (Fig. 3*e*).

We examined the representative MAPK/Akt pathway-associated proteins and cell cycle regulators using Western blotting 72 hr after siRNAs transfection (Fig. 3*f*). Interestingly, phosphorylation of c-Raf, MEK, MAPK, PI3K and pAkt was inhibited by knockdown of *c19orf10*, suggesting the involvement of *c19orf10* in the MAPK/Akt pathways. Furthermore, phosphorylation of Rb, CDK4 and CDK6 was also inhibited by knockdown of *c19orf10*, consistent with the observation of G1 cell cycle arrest by *C19ORF10* knockdown. PTEN, p53 and phosphorylated CDC2 protein expression was not affected by knockdown of *c19orf10*.

C19orf10 encodes the secretory protein and stimulates cell proliferation

As the sequence of *c19orf10* suggested that it encodes a secretory protein, we transfected pSI-*c19orf10-FLAG* in NIH3T3 cells and examined the culture supernatant. Immunoprecipitation of the collected culture supernatant 48 hr after transfection using anti-FLAG antibodies indicated the existence of a 17-kDa protein (c19orf10), compatible with the molecular weight of the 142 amino acids protein encoded by *c19orf10* (Fig. 4*a*). We purified c19orf10-FLAG protein from the supernatant of HEK293 cells infected with Ad. *c19orf10-FLAG* using an anti-FLAG column. Supplementation of purified c19orf10-FLAG into the culture media for 72 hr enhanced the proliferation of HLE cells in a dose-dependent manner with statistical significance, whereas control FLAG peptides

and BSA had no effects on cell proliferation (Fig. 4*b*). Western blot analysis of HLE cells cultured with purified c19orf10-FLAG (40 ng/ml) or BSA control (40 ng/ml) indicated the immediate strong phospholyration of Akt peaked 5 min after supplementation (Fig. 4*c*). The modest phospholyration of GSK3β (Ser9) and p44/42 MAPK also followed and peaked 60 min after c19orf10 supplementation. These data suggest that Akt pathway might be directly involved in the c19orf10-mediated cell proliferation signaling with the subsequent activation of MAPK pathway. Furthermore, addition of antibodies against c19orf10 to the culture media abolished the cell proliferation induced by c19orf10, whereas control IgG had no effects (Fig. 4*d*). Taken together, these data suggest that c19orf10 may be a growth factor overexpressed in AFP-positive HCCs and activates the Akt/MAPK pathways, potentially through the activation of an unidentified c19orf10 receptor.

Discussion

SAGE facilitates the measurement of transcripts from normal and malignant tissues in a nonbiased and highly accurate, quantitative manner. Indeed, SAGE produces a comprehensive gene expression profile without *a priori* gene sequence information, leading to the identification of novel transcripts potentially involved in the pathogenesis of human cancer.[19] In our study, we identified seven SAGE tags potentially corresponding to novel genes activated in HCC. Among them, we identified the secretory protein c19orf10 activated in a subset of HCCs.

Several serum markers including AFP, DCP and Glypican 3 are currently used for the detection and/or the evaluation of the treatment for HCCs in the clinic.[15–18,35] These markers are known as oncofetal proteins, that is, expressed in the fetus, transcriptionally suppressed in the adult organ and reactivated in the tumor. We identified that the expression of *c19orf10* positively correlated with *AFP* expression but did not correlate with the expression of *GPC3* or the biliary marker *KRT19*. As *c19orf10* was rarely detected in the normal liver, it is possible that c19orf10 is also an oncofetal protein activated in HCC. We are currently developing a system to detect serum c19orf10 in HCC patients, and the significance of the serum c19orf10 value as an HCC marker should be clarified.

Recent advancement in molecular biology has revealed the considerable diversity of transcription initiation and/or termination of genes altered in the process of carcinogenesis. Indeed, using 5′ SAGE approach, we recently discovered the novel intronic transcripts activated in HCC.[36] Interestingly, when we investigated the transcription initiation of *c19orf10* using the 5′ SAGE database, we identified a potential 5′ splice variant initiated from the second exon of *c19orf10* (data not shown). Although we have not yet validated the presence of 5′ splice variants in *c19orf10* by PCR, examination of 5′ EST database also suggested the presence of the similar splice variants (GenBank Accession Number CR980295, BQ680744, BQ648461, *etc.*). Alteration of transcription initiation/termination in *c19orf10* might affect the abundance or function of c19orf10 protein, and the details of 5′ splice variants in *c19orf10* should be clarified in future studies.

Molecular targeting therapy has rapidly emerged for solid tumors as well as for leukemia.[37–39] Sorafenib is a multikinase inhibitor targeting Raf kinase in the MAPK pathway as well as VEGFR and the platelet-derived growth factor receptor.[40,41] In our study, we identified that c19orf10 activates the MAPK and Akt/PI3K pathways and contributes to the proliferation of HCC cell lines, although we still could not discover the potential receptor of c19orf10. Development of a neutralizing c19orf10 antibody may provide novel therapeutic options for HCC patients to inhibit these signaling pathways, and its efficacy should be evaluated in the future.

Recently, c19orf10 was found to be expressed in fibroblast-like synoviocytes in the synovium using a proteomics approach.[29] In addition, a recent article indicated that c19orf10 was expressed in preadipocyte cells and involved in adipogenesis using two-dimensional electrophoresis mass spectrometry analysis.[28] Thus, c19orf10 may have pleiotropic effects on various lineages of normal organs in various developmental stages, and the clarification of its distribution and biological properties in the whole body may provide more detailed information about the function of c19orf10.

In conclusion, we have identified the protein c19orf10 that regulates the Akt/MAPK pathways and cell cycle through an unidentified mechanism in HCC. Although further studies should be conducted to detect the potential c19orf10 receptor or signaling molecules binding to c19orf10, our study suggests that c19orf10 may be a novel growth factor, a potential tumor marker and also a potential target molecule for HCC treatment.

Acknowledgements

The authors thank Ms. Mikie Kakiuchi, Ms. Masayo Baba and Ms. Nami Nishiyama for their excellent technical assistance.

References

1. Befeler AS, Di Bisceglie AM. Hepatocellular carcinoma: diagnosis and treatment. *Gastroenterology* 2002;122:1609–19.
2. Tsukuma H, Hiyama T, Tanaka S, Nakao M, Yabuuchi T, Kitamura T, Nakanishi K, Fujimoto I, Inoue A, Yamazaki H, Kawashima T. Risk factors for hepatocellular carcinoma among patients with chronic liver disease. *N Engl J Med* 1993;328:1797–801.
3. Liang TJ, Jeffers LJ, Reddy KR, De Medina M, Parker IT, Cheinquer H, Idrovo V, Rabassa A, Schiff ER. Viral pathogenesis of hepatocellular carcinoma in the United States. *Hepatology* 1993;18:1326–33.
4. Mayans MV, Calvet X, Bruix J, Bruguera M, Costa J, Esteve J, Bosch FX, Bru C, Rodes J. Risk factors for hepatocellular carcinoma in Catalonia, Spain. *Int J Cancer* 1990;46:378–81.

5. Mohamed AE, Kew MC, Groeneveld HT. Alcohol consumption as a risk factor for hepatocellular carcinoma in urban southern African blacks. *Int J Cancer* 1992; 51:537–41.
6. Smedile A, Bugianesi E. Steatosis and hepatocellular carcinoma risk. *Eur Rev Med Pharmacol Sci* 2005;9:291–3.
7. Floreani A, Baragiotta A, Baldo V, Menegon T, Farinati F, Naccarato R. Hepatic and extrahepatic malignancies in primary biliary cirrhosis. *Hepatology* 1999; 29:1425–8.
8. Tradati F, Colombo M, Mannucci PM, Rumi MG, De Fazio C, Gamba G, Ciavarella N, Rocino A, Morfini M, Scaraggi A, Taioli E. A prospective multicenter study of hepatocellular carcinoma in italian hemophiliacs with chronic hepatitis C. The Study Group of the Association of Italian Hemophilia Centers. *Blood* 1998;91:1173–7.
9. Jones DE, Metcalf JV, Collier JD, Bassendine MF, James OF. Hepatocellular carcinoma in primary biliary cirrhosis and its impact on outcomes. *Hepatology* 1997; 26:1138–42.
10. Caballeria L, Pares A, Castells A, Gines A, Bru C, Rodes J. Hepatocellular carcinoma in primary biliary cirrhosis: similar incidence to that in hepatitis C virus-related cirrhosis. *Am J Gastroenterol* 2001; 96:1160–3.
11. Yoshida H, Shiratori Y, Moriyama M, Arakawa Y, Ide T, Sata M, Inoue O, Yano M, Tanaka M, Fujiyama S, Nishiguchi S, Kuroki T, et al. Interferon therapy reduces the risk for hepatocellular carcinoma: national surveillance program of cirrhotic and noncirrhotic patients with chronic hepatitis C in Japan. IHIT Study Group. Inhibition of Hepatocarcinogenesis by Interferon Therapy. *Ann Intern Med* 1999; 131:174–81.
12. Yuen MF, Cheng CC, Lauder IJ, Lam SK, Ooi CG, Lai CL. Early detection of hepatocellular carcinoma increases the chance of treatment: Hong Kong experience. *Hepatology* 2000;31:330–5.
13. Peterson MS, Baron RL. Radiologic diagnosis of hepatocellular carcinoma. *Clin Liver Dis* 2001;5:123–44.
14. Choi BI. The current status of imaging diagnosis of hepatocellular carcinoma. *Liver Transpl* 2004;10:S20–S25.
15. Fujiyama S, Tanaka M, Maeda S, Ashihara H, Hirata R, Tomita K. Tumor markers in early diagnosis, follow-up and management of patients with hepatocellular carcinoma. *Oncology* 2002;62 (Suppl 1):57–63.
16. Tsai SL, Huang GT, Yang PM, Sheu JC, Sung JL, Chen DS. Plasma des-gamma-carboxyprothrombin in the early stage of hepatocellular carcinoma. *Hepatology* 1990; 11:481–8.
17. Ikoma J, Kaito M, Ishihara T, Nakagawa N, Kamei A, Fujita N, Iwasa M, Tamaki S, Watanabe S, Adachi Y. Early diagnosis of hepatocellular carcinoma using a sensitive assay for serum des-gamma-carboxy prothrombin: a prospective study. *Hepatogastroenterology* 2002; 49:235–8.
18. Kasahara A, Hayashi N, Fusamoto H, Kawada Y, Imai Y, Yamamoto H, Hayashi E, Ogihara T, Kamada T. Clinical evaluation of plasma des-gamma-carboxy prothrombin as a marker protein of hepatocellular carcinoma in patients with tumors of various sizes. *Dig Dis Sci* 1993; 38:2170–6.
19. Yamashita T, Honda M, Kaneko S. Application of serial analysis of gene expression in cancer research. *Curr Pharm Biotechnol* 2008;9:375–82.
20. Cheng AL, Kang YK, Chen Z, Tsao CJ, Qin S, Kim JS, Luo R, Feng J, Ye S, Yang TS, Xu J, Sun Y, et al. Efficacy and safety of sorafenib in patients in the Asia-Pacific region with advanced hepatocellular carcinoma: a phase III randomised, double-blind, placebo-controlled trial. *Lancet Oncol* 2009;10:25–34.
21. Llovet JM, Ricci S, Mazzaferro V, Hilgard P, Gane E, Blanc JF, de Oliveira AC, Santoro A, Raoul JL, Forner A, Schwartz M, Porta C, et al. Sorafenib in advanced hepatocellular carcinoma. *N Engl J Med* 2008;359:378–90.
22. Yamashita T, Hashimoto S, Kaneko S, Nagai S, Toyoda N, Suzuki T, Kobayashi K, Matsushima K. Comprehensive gene expression profile of a normal human liver. *Biochem Biophys Res Commun* 2000;269: 110–16.
23. Yamashita T, Honda M, Takatori H, Nishino R, Hoshino N, Kaneko S. Genome-wide transcriptome mapping analysis identifies organ-specific gene expression patterns along human chromosomes. *Genomics* 2004;84:867–75.
24. Yamashita T, Honda M, Takatori H, Nishino R, Minato H, Takamura H, Ohta T, Kaneko S. Activation of lipogenic pathway correlates with cell proliferation and poor prognosis in hepatocellular carcinoma. *J Hepatol* 2009;50:100–10.
25. Yamashita T, Kaneko S, Hashimoto S, Sato T, Nagai S, Toyoda N, Suzuki T, Kobayashi K, Matsushima K. Serial analysis of gene expression in chronic hepatitis C and hepatocellular carcinoma. *Biochem Biophys Res Commun* 2001;282:647–54.
26. Tulin EE, Onoda N, Nakata Y, Maeda M, Hasegawa M, Nomura H, Kitamura T. SF20/IL-25, a novel bone marrow stroma-derived growth factor that binds to mouse thymic shared antigen-1 and supports lymphoid cell proliferation. *J Immunol* 2001;167:6338–47.
27. Tulin EE, Onoda N, Nakata Y, Maeda M, Hasegawa M, Nomura H, Kitamura T. SF20/IL-25, a novel bone marrow stroma-derived growth factor that binds to mouse thymic shared antigen-1 and supports lymphoid cell proliferation. *J Immunol* 2003;170:1593.
28. Wang P, Mariman E, Keijer J, Bouwman F, Noben JP, Robben J, Renes J. Profiling of the secreted proteins during 3T3-L1 adipocyte differentiation leads to the identification of novel adipokines. *Cell Mol Life Sci* 2004;61:2405–17.
29. Weiler T, Du Q, Krokhin O, Ens W, Standing K, El-Gabalawy H, Wilkins JA. The identification and characterization of a novel protein, c19orf10, in the synovium. *Arthritis Res Ther* 2007;9:R30.
30. Takatori H, Yamashita T, Honda M, Nishino R, Arai K, Takamura H, Ohta T, Zen Y, Kaneko S. dUTP pyrophosphatase expression correlates with a poor prognosis in hepatocellular carcinoma. *Liver Int* 2010; 30:438–46.
31. Sakai Y, Honda M, Fujinaga H, Tatsumi I, Mizukoshi E, Nakamoto Y, Kaneko S. Common transcriptional signature of tumor-infiltrating mononuclear inflammatory cells and peripheral blood mononuclear cells in hepatocellular carcinoma patients. *Cancer Res* 2008;68: 10267–79.
32. Honda M, Yamashita T, Ueda T, Takatori H, Nishino R, Kaneko S. Different signaling pathways in the livers of patients with chronic hepatitis B or chronic hepatitis C. *Hepatology* 2006;44:1122–38.
33. Sakai Y, Morrison BJ, Burke JD, Park JM, Terabe M, Janik JE, Forni G, Berzofsky JA, Morris JC. Vaccination by genetically modified dendritic cells expressing a truncated neu oncogene prevents development of breast cancer in transgenic mice. *Cancer Res* 2004;64:8022–8.
34. Sakai Y, Kaneko S, Nakamoto Y, Kagaya T, Mukaida N, Kobayashi K. Enhanced anti-tumor effects of herpes simplex virus thymidine kinase/ganciclovir system by codelivering monocyte chemoattractant protein-1 in hepatocellular carcinoma. *Cancer Gene Ther* 2001;8:695–704.
35. Capurro M, Wanless IR, Sherman M, Deboer G, Shi W, Miyoshi E, Filmus J. Glypican-3: a novel serum and histochemical marker for hepatocellular carcinoma. *Gastroenterology* 2003;125: 89–97.
36. Hodo Y, Hashimoto S, Honda M, Yamashita T, Suzuki Y, Sugano S, Kaneko S, Matsushima K. Comprehensive gene expression analysis of 5′-end of mRNA identified novel intronic transcripts associated with hepatocellular carcinoma. *Genomics* 2010;95:217–23.

37. Romond EH, Perez EA, Bryant J, Suman VJ, Geyer CE, Jr, Davidson NE, Tan-Chiu E, Martino S, Paik S, Kaufman PA, Swain SM, Pisansky TM, et al. Trastuzumab plus adjuvant chemotherapy for operable HER2-positive breast cancer. *N Engl J Med* 2005;353:1673–84.
38. Hurwitz H, Fehrenbacher L, Novotny W, Cartwright T, Hainsworth J, Heim W, Berlin J, Baron A, Griffing S, Holmgren E, Ferrara N, Fyfe G, et al. Bevacizumab plus irinotecan, fluorouracil, and leucovorin for metastatic colorectal cancer. *N Engl J Med* 2004;350:2335–42.
39. Shepherd FA, Rodrigues Pereira J, Ciuleanu T, Tan EH, Hirsh V, Thongprasert S, Campos D, Maoleekoonpiroj S, Smylie M, Martins R, van Kooten M, Dediu M, et al. Erlotinib in previously treated non-small-cell lung cancer. *N Engl J Med* 2005; 353:123–32.
40. Llovet JM, Bruix J. Molecular targeted therapies in hepatocellular carcinoma. *Hepatology* 2008;48:1312–27.
41. Liu L, Cao Y, Chen C, Zhang X, McNabola A, Wilkie D, Wilhelm S, Lynch M, Carter C. Sorafenib blocks the RAF/MEK/ERK pathway, inhibits tumor angiogenesis, and induces tumor cell apoptosis in hepatocellular carcinoma model PLC/PRF/5. *Cancer Res* 2006;66: 11851–8.

Clinical and Experimental Immunology ORIGINAL ARTICLE doi:10.1111/j.1365-2249.2010.04246.x

Prolonged recurrence-free survival following OK432-stimulated dendritic cell transfer into hepatocellular carcinoma during transarterial embolization

Y. Nakamoto,* E. Mizukoshi,* M. Kitahara,* F. Arihara,* Y. Sakai,* K. Kakinoki,* Y. Fujita,* Y. Marukawa,* K. Arai,* T. Yamashita,* N. Mukaida,† K. Matsushima,‡ O. Matsui§ and S. Kaneko*

**Disease Control and Homeostasis, Graduate School of Medicine, †Division of Molecular Bioregulation, Cancer Research Institute, Kanazawa University, §Department of Radiology, Graduate School of Medicine, Kanazawa University, Kanazawa, and ‡Department of Molecular Preventive Medicine, Graduate School of Medicine, University of Tokyo, Tokyo, Japan*

Accepted for publication 19 July 2010
Correspondences: S. Kaneko, Disease Control and Homeostasis, Graduate School of Medical Science, Kanazawa University, 13-1 Takara-machi, Kanazawa 920-8641, Japan.
E-mail: skaneko@m-kanazawa.jp

Summary

Despite curative locoregional treatments for hepatocellular carcinoma (HCC), tumour recurrence rates remain high. The current study was designed to assess the safety and bioactivity of infusion of dendritic cells (DCs) stimulated with OK432, a streptococcus-derived anti-cancer immunotherapeutic agent, into tumour tissues following transcatheter hepatic arterial embolization (TAE) treatment in patients with HCC. DCs were derived from peripheral blood monocytes of patients with hepatitis C virus-related cirrhosis and HCC in the presence of interleukin (IL)-4 and granulocyte-macrophage colony-stimulating factor and stimulated with 0·1 KE/ml OK432 for 2 days. Thirteen patients were administered with 5×10^6 of DCs through arterial catheter during the procedures of TAE treatment on day 7. The immunomodulatory effects and clinical responses were evaluated in comparison with a group of 22 historical controls treated with TAE but without DC transfer. OK432 stimulation of immature DCs promoted their maturation towards cells with activated phenotypes, high expression of a homing receptor, fairly well-preserved phagocytic capacity, greatly enhanced cytokine production and effective tumoricidal activity. Administration of OK432-stimulated DCs to patients was found to be feasible and safe. Kaplan–Meier analysis revealed prolonged recurrence-free survival of patients treated in this manner compared with the historical controls ($P = 0{\cdot}046$, log-rank test). The bioactivity of the transferred DCs was reflected in higher serum concentrations of the cytokines IL-9, IL-15 and tumour necrosis factor-α and the chemokines CCL4 and CCL11. Collectively, this study suggests that a DC-based, active immunotherapeutic strategy in combination with locoregional treatments exerts beneficial anti-tumour effects against liver cancer.

Keywords: dendritic cells, hepatocellular carcinoma, immunotherapy, recurrence-free survival, transcatheter hepatic arterial embolization

Introduction

Many locoregional therapeutic approaches including surgical resection, radiofrequency ablation (RFA) and transcatheter hepatic arterial embolization (TAE) have been taken in the search for curative treatments of hepatocellular carcinoma (HCC). Despite these efforts, tumour recurrence rates remain high [1,2], probably because active hepatitis and cirrhosis in the surrounding non-tumour liver tissues causes *de novo* development of HCC [3,4]. One strategy to reduce tumour recurrence is to enhance anti-tumour immune responses that may induce sufficient inhibitory effects to prevent tumour cell growth and survival [5,6]. Dendritic cells (DCs) are the most potent type of antigen-presenting cells in the human body, and are involved in the regulation of both innate and adaptive immune responses [7]. DC-based immunotherapies are believed to contribute to the eradication of residual and recurrent tumour cells.

To enhance tumour antigen presentation to T lymphocytes, DCs have been transferred with major histocompatibility complex (MHC) class I and class II genes [8] and co-stimulatory molecules, e.g. CD40, CD80 and CD86 [9,10], and loaded with tumour-associated antigens, including tumour lysates, peptides and RNA transfection [11]. To induce natural killer (NK) and natural killer T (NK T) cell activation, DCs have been stimulated and modified to

Table 1. Patient characteristics.

Patient no.	Gender	Age (years)	HLA	TNM stages	No. of tumours	Largest tumour (mm)	Child–Pugh	KPS	Post-TAE Rx
1	M	60	A11 A33	III	5	35	B	100	RFA
2	M	57	A11 A24	III	1	21	B	100	RFA
3	M	57	A11 A31	III	2	39	B	100	RFA
4	M	77	A2 A24	III	2	35	A	100	RFA
5	F	83	A11 A24	III	3	29	B	100	RFA
6	F	74	A2 A24	II	1	35	A	100	RFA
7	F	72	A24 A33	III	3	41	B	100	RFA
8	F	65	A2 A11	II	4	12	B	100	RFA
9	M	71	A2 A11	II	4	16	A	100	RFA
10	M	79	A11 A24	III	2	40	A	100	RFA
11	M	71	A2 A24	II	1	28	A	100	RFA
12	M	56	A2 A26	III	2	25	B	100	RFA
13	M	64	A2 A33	III	2	37	B	100	RFA

M, male; F, female; TNM, tumour–node–metastasis; Child–Pugh, Child–Pugh classification; KPS, Karnofsky performance scores; TAE, transcatheter arterial embolization; Rx, treatment; HCC, hepatocellular carcinoma; HLA, human leucocyte antigen; RFA, percutaneous radiofrequency ablation.

produce larger amounts of cytokines, e.g. interleukin (IL)-12, IL-18 and type I interferons (IFNs)[10,12]. Furthermore, DC migration into secondary lymphoid organs could be induced by expression of chemokine genes, e.g. C-C chemokine receptor-7 (CCR7) [13], and by maturation using inflammatory cytokines [14], matrix metalloproteinases and Toll-like receptor (TLR) ligands [15].

DCs stimulated with OK432, a penicillin-inactivated and lyophilized preparation of *Streptococcus pyrogenes*, were suggested recently to produce large amounts of T helper type 1 (Th1) cytokines, including IL-12 and IFN-γ and enhance cytotoxic T lymphocyte activity compared to a standard mixture of cytokines [tumour necrosis factor-α (TNF-α), IL-1β, IL-6 and prostaglandin E_2 (PGE_2)] [16]. Furthermore, because OK432 modulates DC maturation through TLR-4 and the β_2 integrin system [16,17] and TLR-4-stimulated DCs can abrogate the activity of regulatory T cells [18], OK432-stimulated DCs may contribute to the induction of anti-tumour immune responses partly by reducing the activity of suppressor cells. Recently, in addition to the orchestration of immune responses, OK432-activated DCs have themselves been shown to mediate strong, specific cytotoxicity towards tumour cells via CD40/CD40 ligand interactions [19].

We have reported recently that combination therapy using TAE together with immature DC infusion is safe for patients with cirrhosis and HCC [20]. DCs were infused precisely into tumour tissues and contributed to the recruitment and activation of immune cells *in situ*. However, this approach by itself yielded limited anti-tumour effects due probably to insufficient stimulation of immature DCs (the preparation of which seems closely related to therapeutic outcome [21,22]). The current study was designed to assess the safety and bioactivity of OK432-stimulated DC infusion into tumour tissues following TAE treatment in patients with cirrhosis and HCC. In addition to documenting the safety of this approach, we found that patients treated with OK432-stimulated DCs displayed unique cytokine and chemokine profiles and, most importantly, experienced prolonged recurrence-free survival.

Patients and methods

Patients

Inclusion criteria were a radiological diagnosis of primary HCC by computed tomography (CT) angiography, hepatitis C virus (HCV)-related HCC, a Karnofsky score of $\geq$ 70%, an age of $\geq$ 20 years, informed consent and the following normal baseline haematological parameters (within 1 week before DC administration): haemoglobin $\geq$ 8·5 g/dl; white cell count $\geq$ 2000/μl; platelet count $\geq$ 50 000/μl; creatinine $<$ 1·5 mg/dl and liver damage A or B [23].

Exclusion criteria included severe cardiac, renal, pulmonary, haematological or other systemic disease associated with a discontinuation risk; human immunodeficiency virus (HIV) infection; prior history of other malignancies; history of surgery, chemotherapy or radiation therapy within 4 weeks; immunological disorders including splenectomy and radiation to the spleen; corticosteroid or anti-histamine therapy; current lactation; pregnancy; history of organ transplantation; or difficulty in follow-up.

Thirteen patients (four women and nine men) presenting at Kanazawa University Hospital between March 2004 and June 2006 were enrolled into the study, with an age range from 56 to 83 years (Table 1). Patients with verified radiological diagnoses of HCC stage II or more were eligible and enrolled in this study. In addition, a group of 22 historical controls (nine women and 13 men) treated with TAE without DC administration between July 2000 and September 2007 was included in this study. All patients received RFA therapy to increase the locoregional effects 1 week later [24].

They underwent ultrasound, computed tomography (CT) scan or magnetic resonance imaging (MRI) of the abdomen about 1 month after treatment and at a minimum of once every 3 months thereafter, and tumour recurrences were followed for up to 360 days. The Institutional Review Board reviewed and approved the study protocol. This study complied with ethical standards outlined in the Declaration of Helsinki. Adverse events were monitored for 1 month after the DC infusion in terms of fever, vomiting, abdominal pain, encephalopathy, myalgia, ascites, gastrointestinal disorder, bleeding, hepatic abscess and autoimmune diseases.

Preparation and injection of autologous DCs

DCs were generated from blood monocyte precursors, as reported previously [25]. Briefly, peripheral blood mononuclear cells (PBMCs) were isolated by centrifugation in Lymphoprep™ Tubes (Nycomed, Roskilde, Denmark). For generating DCs, PBMCs were plated in six-well tissue culture dishes (Costar, Cambridge, MA, USA) at $1{\cdot}4 \times 10^7$ cells in 2 ml per well and allowed to adhere to plastic for 2 h. Adherent cells were cultured in serum-free media (GMP CellGro® DC Medium; CellGro, Manassas, VA, USA) with 50 ng/ml recombinant human IL-4 (GMP grade; CellGro®) and 100 ng/ml recombinant human granulocyte–macrophage colony-stimulating factor (GM-CSF) (GMP grade; CellGro®) for 5 days to generate immature DC, and matured for a further 2 days in 0·1 KE/ml OK432 (Chugai Pharmaceuticals, Tokyo, Japan) to generate OK-DC. On day 7, the cells were harvested for injection, 5×10^6 cells were suspended in 5 ml normal saline containing 1% autologous plasma, mixed with absorbable gelatin sponge (Gelfoam; Pharmacia & Upjohn, Peapack, NJ, USA) and infused through an arterial catheter following Lipiodol (iodized oil) (Lipiodol Ultrafluide, Laboratoire Guerbet, Aulnay-Sous-Bois, France) injection during selective TAE therapy. Release criteria for DCs were viability > 80%, purity > 30%, negative Gram stain and endotoxin polymerase chain reaction (PCR) and negative in process cultures from samples sent 48 h before release. All products met all release criteria, and the DCs had a typical phenotype of $CD14^-$ and human leucocyte antigen (HLA)-DR^+.

Flow cytometry analysis

The DC preparation was assessed by staining with the following monoclonal antibodies for 30 min on ice: anti-lineage cocktail 1 (lin-1; CD3, CD14, CD16, CD19, CD20 and CD56)-fluorescein isothiocyanate (FITC), anti-HLA-DR-peridinin chlorophyll protein (PerCP) (L243), anti-CCR7-phycoerythrin (PE) (3D12) (BD PharMingen, San Diego, CA, USA), anti-CD80-PE (MAB104), anti-CD83-PE (HB15a) and anti-CD86-PE (HA5.2B7) (Beckman Coulter, Fullerton, CA, USA). Cells were analysed on a fluorescence activated cell sorter (FACS0Calibur™ flow cytometer. Data analysis was performed with CELLQuest™ software (Becton Dickinson, San Jose, CA, USA).

DC phagocytosis

Immature DCs and OK432-stimulated DCs were incubated with 1 mg/ml FITC dextran (Sigma-Aldrich, St Louis, MO, USA) for 30 min at 37°C and the cells were washed three times in FACS buffer before cell acquisition using a FACS-Calibur™ cytometer. Control DCs (not incubated with FITC dextran) were acquired at the same time to allow background levels of fluorescence to be determined.

Enzyme-linked immunosorbent assay (ELISA)

DCs were seeded at 200 000 cells/ml, and supernatant collected after 48 h. IL-12p40 and IFN-γ were detected using matched paired antibodies (BD Pharmingen) following standard protocols.

Cytotoxicity assays

The ability of DCs to exert cytotoxicity was assessed in a standard ^{51}Cr release assay [19]. We used the HCC cell lines Hep3B and PLC/PRF/5 [American Type Culture Collection (ATCC), Manassas, VA, USA] and a lymphoblastoid cell line T2 that expresses HLA-A*0201 (ATCC) as target cells. Target cells were labelled with ^{51}Cr. In a 96-well plate, $2{\cdot}5 \times 10^3$ target cells per well were incubated with DCs for 8 h at different effector/target (E/T) ratios in triplicate. Percentage of specific lysis was calculated as follows: (experimental release – spontaneous release)/(maximum release – spontaneous release) × 100. Spontaneous release was always < 20% of the total.

NK cell activity

NK cell cytotoxicity against K562 erythroleukemia target cells was measured by using ^{51}Cr-release assay, according to previously published methods [26], with PBMCs obtained from the patients. All experiments were performed in triplicate. Percentage of cytotoxicity was calculated as follows: {[experimental counts per minute (cpm) – spontaneous cpm]/[total cpm – spontaneous cpm]} × 100.

Intracellular cytokine expression

Freshly isolated PBMCs were stimulated with 25 ng/ml phorbol 12-myristate 13-acetate (PMA; Sigma-Aldrich) and 1 μg/ml ionomycin (Sigma-Aldrich) at 37°C in humidified 7% CO_2 for 4 h. To block cytokine secretion, brefeldin A (Sigma) [27] was added to a final concentration of 10 μg/ml. After addition of stimuli, the surface staining was performed with anti-CD4-PC5 (13B8·2), anti-CD8-PerCP (SK1) and anti-CD56-PC5 (N901) (Beckman

Coulter). Subsequently, the cells were permeabilized, stained for intracellular IFN-γ and IL-4 using the FastImmune™ system (BD Pharmingen), resuspended in phosphate-buffered saline (PBS) containing 1% paraformaldehyde (PFA), and analysed on a flow cytometer (≈ 10 000 gated events acquired per sample).

IFN-γ enzyme-linked immunospot (ELISPOT) assay

ELISPOT assays were performed as described previously with the following modifications [28–30]. HLA-A24 restricted peptide epitopes, squamous cell carcinoma antigen recognized by T cells 2 $(SART2)_{899}$ (SYTRLFLIL), $SART3_{109}$ (VYDYNCHVDL), multi-drug resistance protein 3 $(MRP3)_{765}$ (VYSDADIFL), $MRP3_{503}$ (LYAWEPSFL), $MRP3_{692}$ (AYVPQQAWI), alpha-fetoprotein $(AFP)_{403}$ (KYIQESQAL), AFP_{434} (AYTKKAPQL), AFP_{357} (EYSRRHPQL), human telomerase reverse transcriptase $(hTERT)_{167}$ (AYQVCGPPL) (unpublished), $hTERT_{461}$ (VYGFVRACL) and $hTERT_{324}$ (VYAETKHFL) were used in this study. Negative controls consisted of an HIV envelope-derived peptide ($HIVenv_{584}$). Positive controls consisted of 10 ng/ml PMA (Sigma) or a CMV pp65-derived peptide ($CMVpp65_{328}$). The coloured spots were counted with a KS ELISPOT Reader (Zeiss, Tokyo, Japan). The number of specific spots was determined by subtracting the number of spots in the absence of antigen from the number of spots in its presence. Responses were considered positive if more than 10 specific spots were detected and if the number of spots in the presence of antigen was at least twofold greater than the number of spots in the absence of antigen.

Cytokine and chemokine profiling

Serum cytokine and chemokine levels were measured using the Bioplex assay (Bio-Rad, Hercules, CA, USA). Briefly, frozen serum samples were thawed at room temperature, diluted 1:4 in sample diluents, and 50 µl aliquots of diluted sample were added in duplicate to the wells of a 96-well microtitre plate containing the coated beads for a validated panel of 27 human cytokines and chemokines (cytokine 27-plex antibody bead kit) according to the manufacturer's instructions. These included IL-1β, IL-1Ra, IL-2, IL-4, IL-5, IL-6, IL-7, IL-8, IL-9, IL-10, IL-12p70, IL-13, IL-15, IL-17, basic fibroblast growth factor (FGF), eotaxin, G-CSF, GM-CSF, IFN-γ, interferon gamma-induced protein (IP)-10, monocyte chemoattractant protein (MCP)-1, MIP-1α, MIP-1β, platelet-derived growth factor (PDGF)-BB, regulated upon activation normal T cell-expressed and secreted (RANTES), TNF-α and vascular endothelial growth factor (VEGF). Eight standards (ranging from 2 to 32 000 pg/ml) were used to generate calibration curves for each cytokine. Data acquisition and analysis were performed using Bio-Plex Manager software version 4.1.1.

Arginase activity

Serum samples were tested for arginase activity by conversion of L-arginine to L-ornithine [31] using a kit supplied by the manufacturer (BioAssay Systems, Hayward, CA, USA). Briefly, sera were treated with a membrane filter (Millipore, Billerica, MA, USA) to remove urea, combined with the sample buffer in wells of a 96-well plate, and incubated at 37°C for 2 h. Subsequently, the urea reagent was added to stop the arginase reaction. The colour produced was read at 520 nm using a microtitre plate reader.

Statistical analysis

Results are expressed as means ± standard deviation (s.d.). Differences between groups were analysed for statistical significance by the Mann–Whitney *U*-test. Qualitative variables were compared by means of Fisher's exact test. The estimated probability of tumour recurrence-free survival was determined using the Kaplan–Meier method. The Mantel–Cox log-rank test was used to compare curves between groups. Any *P*-values less than 0·05 were considered statistically significant. All statistical tests were two-sided.

Results

Preparation of OK432-stimulated DCs

Adherent cells isolated from PBMCs of patients with cirrhosis and HCC (Table 1) were differentiated into DCs in the presence of IL-4 and GM-CSF. The cells were stimulated with 0·1 KE/ml OK432 for 3 days; 54·6 ± 9·5% (mean ± s.d.; $n = 13$) of OK432-stimulated cells showed high levels of MHC class II (HLA-DR) and the absence of lineage markers including CD3, CD14, CD16, CD19, CD20 and CD56, in which 30·9 ± 14·2% were CD11c-positive (myeloid DC subset) and 14·8 ± 11·2 were CD123-positive (plasmacytoid DC subset), consistent with our previous observations [20]. As reported [32,33], greater proportions of the cells developed high levels of expression of the co-stimulatory molecules B7-1 (CD80) and B7-2 (CD86) and an activation marker (CD83) compared to DCs prepared without OK432 stimulation (Fig. 1a). Furthermore, the chemokine receptor CCR7 which leads to homing to lymph nodes [13,34] was also induced following OK432 stimulation.

To evaluate the endocytic and phagocytic ability of the OK432-stimulated cells, uptake of FITC-dextran was quantitated by flow cytometry (Fig. 1b). The cells showed lower levels of uptake due to maturation compared to DCs prepared without OK432 stimulation, while the OK432-stimulated cells derived from HCC patients preserved a moderate uptake capacity. As expected, the OK432-stimulated cells produced large amounts of cytokines IL-12 and IFN-γ (Fig. 1c). In addition, they displayed high cyto-

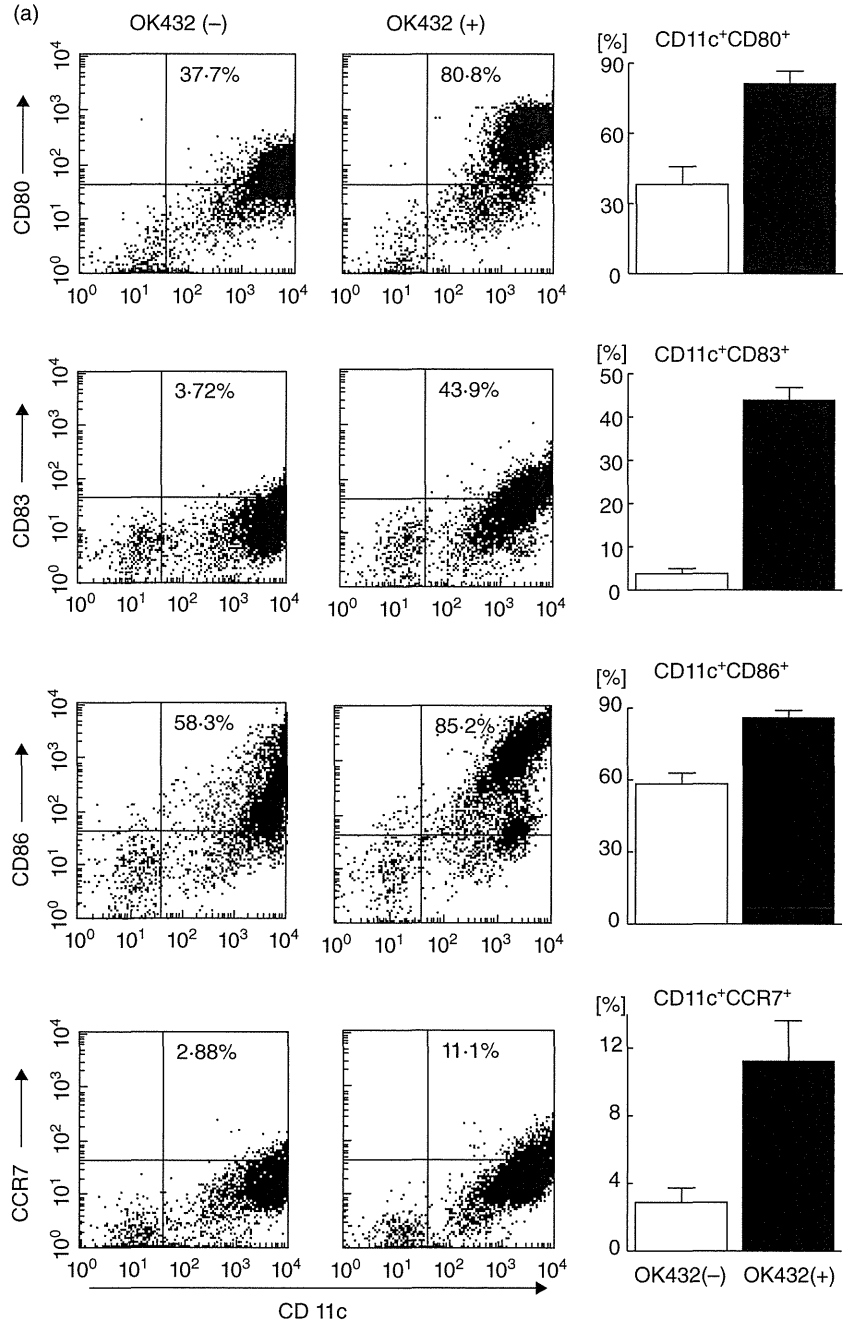

Fig. 1. Effects of OK432 stimulation on the properties of dendritic cells (DCs) generated from blood monocyte precursors in patients with cirrhosis and hepatocellular carcinoma (HCC) ($n = 13$). (a) Lineage cocktail 1 (lin 1^-) human leucocyte antigen D-related (HLA-DR^-) subsets with [OK432($^+$)] and without [OK432($^-$)] stimulation were analysed for surface expression of CD80, CD83, CD86 and CCR7. Dot plots of a representative case are shown in the left-hand panel. Mean percentages [±standard deviation (s.d.)] of positive cells are indicated in the right-hand panel. OK432 stimulation resulted in the expression of high levels of CD80, CD83, CD86 and CCR7 in the lin 1^-human leucocyte antigen D-related (HLA-DR^-) DC subset. (b) DC subsets with and without OK432 stimulation were incubated with fluorescein isothiocyanate (FITC) dextran for 30 min and the uptake was determined by flow cytometry. A representative analysis is shown in the upper panel. Mean fluorescence intensities (MFIs) (±s.d.) of the positive cells are indicated in the lower panel. OK432-stimulated cells showed lower levels of uptake due to maturation. (c) DC supernatants were harvested and the concentrations of interleukin (IL)-12 and interferon (IFN)-γ measured by enzyme-linked immunosorbent assay (ELISA). OK432-stimulated cells produced large amounts of the cytokines. The data indicate means ± s.d. of the groups with and without the stimulation. All comparisons in (a–c) [OK432(+) *versus* OK432($^-$)] were statistically significant by the Mann-Whitney *U*-test ($P < 0{\cdot}005$). (d) Tumoricidal activity of DCs assessed by incubation with ^{51}Cr-labelled Hep3B, PLC/PRF/5 and T2 targets for 8 h at the indicated effector/target (E/T) cell ratios. OK432-stimulated cells displayed high cytotoxic activity against the target cells. The results are representative of the cases studied.

toxic activity against HCC cell lines (Hep3B and PLC/PRF/5) and a lymphoblastoid cell line (T2) although DCs without OK432 stimulation lysed none of the target cells to any great degree (Fig. 1d). Taken together, these results demonstrate that OK432 stimulation of IL-4 and GM-CSF-induced immature DCs derived from HCC patients promoted their maturation towards cells with activated phenotypes, high expression of a homing receptor, fairly well-preserved phagocytic capacity, greatly enhanced cytokine production and effective tumoricidal activity, consistent with previous observations [16,19].

Safety of OK432-stimulated DC administration

Prior to the administration of OK432-stimulated DCs to patients, the cells were confirmed to be safe in athymic nude mice to which 100-fold cell numbers/weight were injected subcutaneously (data not shown). Subsequently, OK432-stimulated DC administration was performed during TAE therapy in humans, in which DCs were mixed together with absorbable gelatin sponge (Gelfoam) and infused through an arterial catheter following iodized oil (Lipiodol) injection, as reported previously [20]. Adverse events were

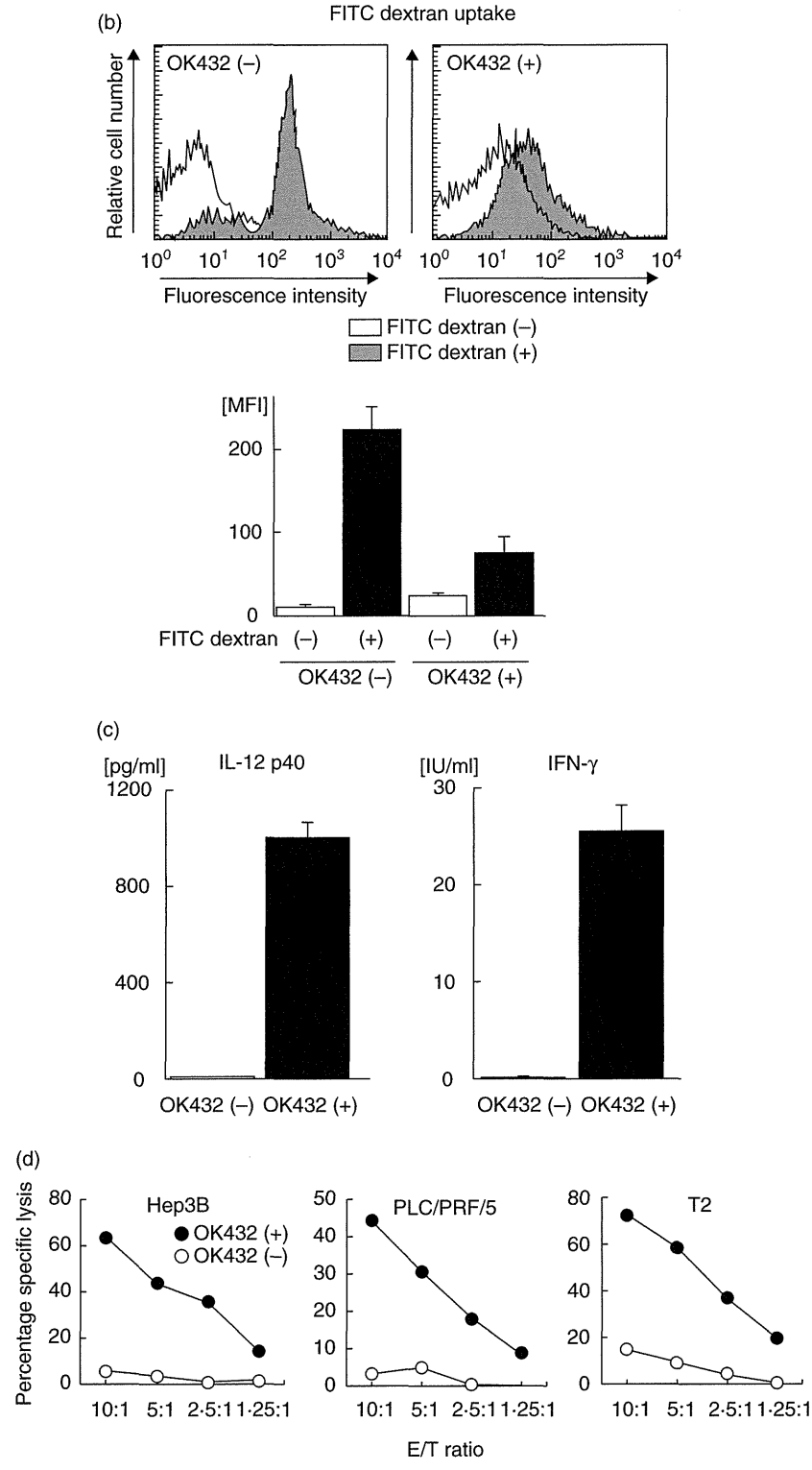

Fig. 1. *Continued*

monitored clinically and biochemically after DC infusion (Table 2). A larger proportion (12 of 13) of the patients were complicated with high fever compared to those treated previously with immature DCs (five of 10) [20], due probably to the proinflammatory responses induced by OK432-stimulated DCs. However, there were no grades III or IV National Cancer Institute Common Toxicity Criteria adverse events, including vomiting, abdominal pain, encephalopathy, myalgia, ascites, gastrointestinal disorders, bleeding, hepatic abscess or autoimmune diseases associated with DC infusion and TAE in this study. There was also no clinical or serological evidence of hepatic failure or autoimmune

Table 2. Adverse events.

Patient no.	Fever (days)	Vomiting	Abdominal pain	Encephalopathy	Others†
1	2	No	No	No	No
2	2	No	No	No	No
3	1	No	No	No	No
4	3	No	No	No	No
5	3	No	No	No	No
6	4	No	No	No	No
7	10	No	No	No	No
8	No	No	No	No	No
9	2	No	No	No	No
10	1	No	No	No	No
11	2	No	No	No	No
12	2	No	No	No	No
13	1	No	No	No	No

†Other adverse events include myalgia, ascites, gastrointestinal disorder, bleeding, hepatic abscess and autoimmune diseases.

response in any patients. Thus, concurrent treatment with OK432-stimulated DC infusions can be performed safely at the same time as TAE in patients with cirrhosis and HCC.

Recurrence-free survival following DC infusion

A further objective of this study was to determine clinical response following DC infusion. A group of historical controls treated with TAE without DC administration was reviewed for this study (Table 3). The clinical characteristics including tumour burden and hepatic reserve were comparable between patients treated with TAE and OK432-stimulated DC transfer ($n = 13$) and those historical controls with TAE but without DC administration ($n = 22$). We compared the recurrence-free survival between these patient groups. Kaplan–Meier analysis indicated that patients treated with TAE and OK432-stimulated DC transfer had prolonged recurrence-free survival compared with the historical controls that had been treated with TAE alone (recurrence rates 360 days after the treatments; two of 13 and 12 of 22, respectively; $P = 0{\cdot}046$, log-rank test) (Fig. 2). The results demonstrated that OK432-stimulated DC transfer during TAE therapy reduces tumour recurrence in HCC patients.

NK cell activity and intracellular cytokine responses in PBMCs

To assess systemic immunomodulatory effects of OK432-stimulated DC transfer, PBMCs were isolated 1 and 3 months after treatment and NK cell cytotoxicity against K562 erythroleukaemia target cells measured using the ^{51}Cr-release assay (Fig. 3). The level of NK cell was unaltered following treatment. In addition, cytokine production capacity of lymphocyte subsets was quantitated by measuring intracellular IFN-γ and IL-4 using flow cytometry. There were also no significant changes in terms of cytokine production capacity in the $CD4^+$, $CD8^+$ and $CD56^+$ subsets in the patients treated with OK432-stimulated DCs.

Immune responses to peptide epitopes derived from tumour antigens

To assess the effects on T cell responses to tumour antigens, PBMCs were obtained 4 weeks after DC infusion, pulsed with peptides derived from AFP, MRP3, SART2, SART3 and hTERT. IFN-γ production was then quantitated in an

Table 3. Clinical characteristics of patients treated with TAE + OK-DC and TAE alone.

	TAE + OK-DC	TAE	*P*
No. of patients	13	22	
Age (years)	68.2 ± 9.1	70.0 ± 7.6	n.s.†
Gender (M/F)	9/4	13/9	n.s.‡
White cell count ($\times 10^2/\mu l$)	34.4 ± 11.6	41.4 ± 18.9	n.s.†
Lymphocytes ($\times 10^2/\mu l$)	10.4 ± 3.6	12.4 ± 4.7	n.s.†
Platelets ($\times 10^4/\mu l$)	11.5 ± 10.2	10.3 ± 5.8	n.s.†
Hepaplastin test (%)	64.6 ± 11.6	75.5 ± 24.3	n.s.†
ALT (IU/l)	56.7 ± 38.9	67.9 ± 44.6	n.s.†
Total bilirubin (mg/dl)	1.3 ± 0.7	1.1 ± 0.6	n.s.†
Albumin (g/dl)	3.4 ± 0.6	3.6 ± 0.4	n.s.†
Non-cancerous liver parenchyma (no.)			
Chronic hepatitis	0	8	
Cirrhosis (Child–Pugh A/B/C)	13 (5/8/0)	14 (6/8/0)	n.s.‡
TNM stages (I/II/III/IV-A/IV-B)	0/4/9/0/0	3/8/11/0/0	n.s.‡
No. of tumours	2.5 ± 1.3	1.9 ± 1.3	n.s.†
Largest tumour (mm)	30.2 ± 9.4	32.6 ± 15.2	n.s.†
AFP	204.8 ± 404.1	201.8 ± 544.2	n.s.†

Results are expressed as means ± standard deviation. †Mann–Whitney *U*-test. ‡Fisher's exact test. TAE, transcatheter arterial embolization; OK-DC, OK432-stimulated dendritic cells; ALT, alanine transaminase; TNM, tumour–node–metastasis; AFP, alpha-fetoprotein; Child–Pugh, Child–Pugh classification; n.s., not significant.